Chemical Engineering Journal 527 (2026) 172045

Contents lists available at ScienceDirect

Chemical Engineering Journal

journal homepage: www.elsevier.com/locate/cej

Performance comparison and sustainability assessment of mesoporous FAU zeolites for the plastic upcycling

Muhammad Usman Azam [a,b], Nanbyen George Kim [a], Auguste Fernandes [c], M. Filipa Ribeiro [c], Waheed Afzal [a,*], Inês Graça [a,*]

[a] Chemical Processes and Materials Group, School of Engineering, University of Aberdeen, Aberdeen, AB24 3UE, Scotland, UK
[b] School of Engineering, Cardiff University, CF24 3AA, Cardiff, UK
[c] Centro de Química Estrutural, Institute of Molecular Sciences, Instituto Superior Técnico, Universidade de Lisboa, Av. Rovisco Pais, 1049-001, Lisboa, Portugal

ARTICLE INFO

Keywords:
Hydrocracking
Hierarchical zeolites
Top-down templating
Bottom-up templating
Sustainability assessment

ABSTRACT

This study investigates the influence of hierarchical modification of zeolites, synthesized via top-down (surfactant-templating via basic solution of CTAB) and bottom-up (use of organosilane, TPOAC) approaches, on the hydrocracking of linear and branched chain plastics. Unlike traditional comparisons exclusively based on catalytic performance, this study further provides an insight into the simultaneous comparison of conversion with environmental and economic benefits. Overall, top-down hierarchical zeolites (CT-HY) showed higher conversions than bottom-up modified (ST-HY) and HY zeolites for the hydrocracking of virgin HDPE and mixed post-consumer plastic waste, suggesting that improved textural properties play a dominant role for the hydrocracking of plastics. Interestingly, while conversion increases progressively with mesoporosity when branched plastics are present, a plateau in conversion is reached after a certain mesoporosity development for linear-chain plastics. However, product quality improves steadily with the increase in mesoporosity in both cases. A 27 % higher Pareto front optimisation score was obtained for the prolonged treated top-down hierarchical HY zeolite (CT-HY-2) than HY when processing mixed post-consumer plastic waste. Finally, the sustainability assessment showed the benefits of top-down hierarchically modified Y zeolites as compared to previous literature, with both zeolites showing high productivity of middle distillates (6.96–8.35 $g_{C5\text{-}C18}\ g_{cat}^{-1}\ h^{-1}$).

Overall, the present study shows the contribution of mesoporosity in hierarchical zeolites to the upcycling of different types of plastic chains. Similarly, the demonstration of sustainability assessment helps to optimise the physiochemical properties of hierarchical zeolites and reaction conditions for improved catalytic results and provides decision makers a standardised approach when studying industrial-scale processes.

1. Introduction

The growing demand for single-use plastics, coupled with plastic waste generation and mismanagement, has resulted in an adverse impact on our environment and climate change. Globally, 391 million metric tonne (Mt) of plastic waste were generated in 2021, with the projected value to reach 687 Mt by 2050 [1,2]. The lower recycling rate (~9 %) combined with the maximum disposal of plastic waste into landfills (>50 %) are resulting in significant economic loss [3]. In response, a resolution was passed in 2022 to establish an international legally enforceable United Nations (UN) treaty to combat plastic pollution by increasing the plastic recycling rate to 80 % by 2040 [4]. However, the use of traditionally circular approaches, i.e., mechanical recycling, and thermochemical recycling (i.e., gasification, and pyrolysis), unsustainably contribute towards plastic circularity, as these methods are either energy intensive and/or downcycle the plastic feedstock to low-value products [5,6]. In contrast, hydrocracking has recently emerged as an alternative approach to pyrolysis and gasification, and has the potential to reduce the energy requirements while producing valuable products [7,8].

Recent efforts have focused on the use of acid catalysts including sulfated-zirconia (i.e., SO_4/ZrO_2-Al_2O_3 [9]), zeolites (i.e., HY [5], Hβ [6], HZSM-5 [7], and layered self-pillared HZSM-5 [10]), dual-catalysts (i.e., WZr-KIT-6 + HZSM-5 and Pt/Al_2O_3 + Y [11]), metal supported catalysts (i.e., AC-Mn(5)/Zn(5) [12], Pt/C [13], Ru/C [14], and Mn-Al_2O_3 [15]), and/or bi-functional metal-acid catalysts (Ni-HY [5] and

* Corresponding authors.
E-mail addresses: waheed@abdn.ac.uk (W. Afzal), i.graca@abdn.ac.uk (I. Graça).

https://doi.org/10.1016/j.cej.2025.172045
Received 23 September 2025; Received in revised form 3 December 2025; Accepted 17 December 2025
Available online 23 December 2025

Pt/HY [16]) for the hydrocracking of waste plastics to improve the conversion and selectivity of desired products as compared to the purely thermal hydrocracking. However, the low thermal stability and loss of sulphur content at elevated temperatures limit the applications of sulphated zirconia towards plastic hydrocracking. Similarly, dual catalysts and metal-supported catalysts either show weak acidity and/or require prolonged reaction time (24–72 h) to crack plastics, thereby limiting their industrial applications. In contrast, zeolites have been demonstrating exceptional results owing to their acidity, crystallinity and defined porous structure. Despite this, the microporosity of conventional zeolites limits the diffusion of bulkier polymeric molecules towards the internal active sites, resulting in pore blockage, low conversion, and eventually catalyst deactivation [5]. This could be resolved by engineering the textural properties of the zeolites to hierarchical pore structures, thereby improving the accessibility of polymeric feedstock and their reaction intermediates to the active sites of the zeolite, resulting in an increase in conversion [17].

Overall, a wide range of modification routes (i.e., top-down and bottom-up) has been studied and used to develop hierarchical zeolites [18–20]. Fig. 1a shows a simplified map to illustrate the effect of different hierarchical modifications on the parent zeolite. This simplified, qualitative map is not intended to represent the exact acidity and functionality of zeolites and will not focus on all pertinent parameters (i.e., Si/Al of parent zeolite, type of zeolite, and synthesis conditions, etc.), but rather offers a framework to discuss general possibilities during the hierarchical modification of zeolites. For instance, steaming Y zeolite at high temperatures improves its textural properties and stability but often reduces crystallinity, and alters the Si/Al ratio. Similarly, a single steaming step is usually insufficient to improve the textural properties of microporous zeolites, and the need for 2–3 steaming cycles makes the process energy-intensive, contributing significantly for global warming potential (~2 kg CO_2e g^{-1}) [5]. Moreover, desilication and acid leaching of zeolites are responsible for introducing uncontrollable porosity via zeolite-dissolution, thereby significantly altering the Si/Al of the parent zeolite [21–23]. Similarly, these hierarchical modification techniques are highly influenced by the Si/Al ratio of the parent zeolite. In addition, the use of hard templating and zeolitization approaches may lead to a reduction in the crystallinity of the hierarchical zeolite [8,24], resulting a detrimental impact on the crystallinity, stability, and eventually catalytic properties of hierarchical zeolites [25]. In contrast, bottom-up (soft-templating) and and/or top-down (surfactant-templating) approaches result in well-embedded and uniform mesoporosity because the micelles act as ordered structure-directing agents, producing well-defined pore sizes without zeolite dissolution [26,27]. The bottom-up and top-down synthesis of zeolites by using long-chain alkylammonium moieties demonstrated enhanced acidity, even without altering their Si/Al ratios (Fig. 1a). Fig. 1b shows a comparison between the textural and acidic properties of hierarchical zeolites synthesized via surfactant-templating and soft-templating and those previously reported in literature.

Recently, Kots et al. [25] synthesized a hierarchical Mordenite (HyMOR) (via top-down approach using CTAB) with intercrystalline mesoporosity. Interestingly, HyMOR showed high conversion of HDPE (83.6 %) as compared to the parent MOR (33 %), owing to its improved mesoporosity (+145 %) and acidity (+32 % increase). Nevertheless, if the modification process is not controlled, it results in loss of

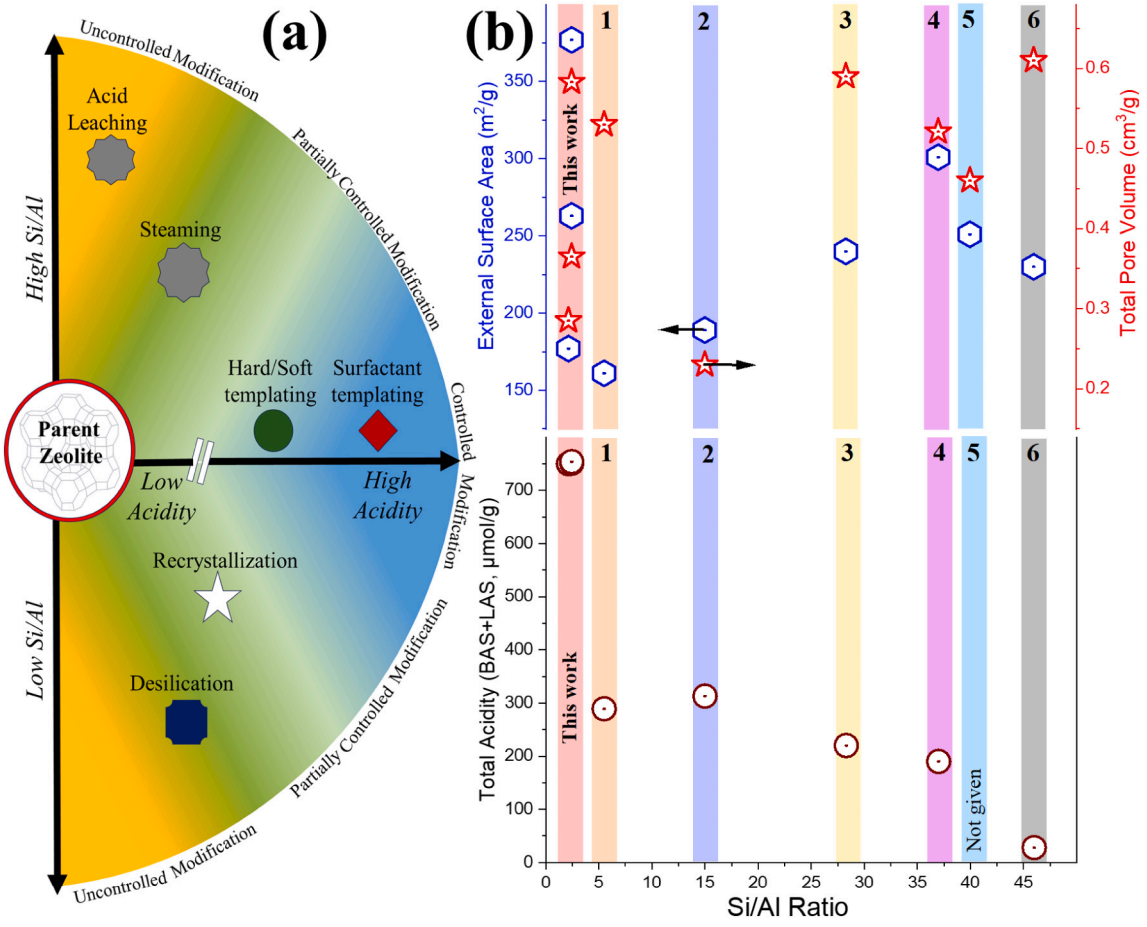

Fig. 1. Comparison of different hierarchical modification approaches with the current study: (a) Simplified map to illustrate the effect of different hierarchical modification techniques on the functionality and acidity of zeolites, (b) effect on the textural properties and total acidity of zeolite samples in comparison to previous literature. The numbers from 1 to 6 correspond to ref. [21], ref. [31], ref. [32], ref. [5], ref. [33] and ref. [32], respectively.

crystallinity and catalytic activity, as observed by Tan et al. [17] while synthesizing surfactant-templated Y zeolites with different Si/Al ratios (Si/Al = 15 and 40) and studying them for the hydrocracking of PE. Both hierarchical Y zeolite samples presented enhanced textural properties, but exhibited lower activity than their parent counterparts, due to a loss in crystallinity. The authors also hypothesized that the parent Y zeolites already had significant mesoporosity (V_{meso} = 0.18–0.20 $cm^3\ g^{-1}$) to allow initiating the diffusion of bulkier PE molecules into the zeolite framework, and a further enhancement of the mesopore volume (V_{meso} = 0.40–0.77 $cm^3\ g^{-1}$) did not influence the conversion. Moreover, Ryoo et al. [28] confirmed the advantages of using hierarchical MFI zeolite synthesized via bottom-up approach using $C_{22\text{-}6\text{-}6}Br_2$ surfactant for the improved cracking of HDPE (85 %), owing to its high textural properties as compared to a conventional MFI zeolite (27 %). Similar results were reported by Song et al. [29] who synthesized a hierarchical MFI using mesoporogen soft template ($C_{24}H_{57}O_{13}NSi_3$) and studied it for the cracking of LDPE. The hierarchical zeolite exhibited better cracking ability of LDPE as compared to the microporous zeolite, confirming the significance of better textural and acidic properties for improved catalytic properties. Although the individual benefits of bottom-up and top-down hierarchical modification routes using different surfactants for the hydrocracking of plastics have been reported in literature [11,17,25,29,30], there have been no documented studies comparing the use of mesoporous zeolites synthesized via selected top-down and bottom-up approaches, by using different long chain alkylammonium moieties, for this application. In addition, the impact of their pore architectures and pore connectivity towards the diffusion of different plastic feedstocks remains fairly unexplored. Moreover, the catalytic hydrocracking process has never been optimized in terms of the trade-offs between the economic and environmental benefits, thereby overlooking the sustainability of the obtained product distribution. Similarly, the previous literature primarily focused on the ease of developing hierarchical zeolite through post-modification approaches, without adequately addressing and comparing the associated environmental and economic consequences.

Herein, we synthesized a microporous HY zeolite via hydrothermal synthesis, and various hierarchical zeolites via bottom-up (using dimethyl octadecyl-(3-trimethoxysilylpropyl)-ammonium chloride, TPOAC) and top-down (using cetyltrimethylammonium bromide, CTAB) approaches. Both surfactants (i.e., TPOAC and CTAB) are quite inexpensive, widely available and result in highly controlled porosity as compared to their substitutes (i.e., CTEAB, P123, and F127, etc.). The effect of hierarchical modification of various zeolites was studied at different reaction temperatures (325–390 °C) for 1 h under 30 bar cold H_2 pressure during the hydrocracking of both linear and branched polymers. Similarly, we discussed the role of textural and acidic properties of zeolites towards the product distribution during the hydrocracking experiments. Furthermore, the activity of the various zeolites were compared and optimized based on a simple Pareto front methodology by normalizing their conversion score and the environmental and economic benefits of their product distribution. Finally, the sustainability assessment of the hydrocracking process was performed by following the principles of green chemistry. This included a comparison of the productivity of middle distillates (C_5-C_{18}) and the environmental and economic costs of the synthesized catalysts with previously reported zeolite materials. Overall, the present study aims to provide an insight into the development of sustainable hierarchical zeolites and explain the role of mesoporosity of hierarchical zeolites towards the hydrocracking of different plastics. Also, the comparison of various zeolites based on their conversion, environmental and economic scores unlocks the understanding of the balance required to truly achieve the sustainability of the process.

2. Materials and methods

2.1. Synthesis of Y zeolite (HY)

For the synthesis of the Y zeolite, known quantities of NaOH (4.6 g) and $NaAlO_2$ (2 g) were added to 29 ml of deionised (DI) water under stirring until a clear solution was achieved. In the next step, 19 g of colloidal silica was added dropwise to the above solution under vigorous stirring. The resulting solution was stirred for another 2 h, then transferred into a 60 ml polypropylene (PP) bottle and placed in an oven at 90 °C for 24 h. The composition of the resulting gel was 12 SiO_2: Al_2O_3: 6.7 Na_2O: 220 H_2O. After 24 h, the bottle was cooled down to room temperature, and the product was filtered and washed with DI water to remove any unreacted precursors. The filtered powder was dried in an oven at 100 °C overnight and represented as NaY (sodium form of Y zeolite). Additionally, the NaY sample was subjected to three successive ion-exchanges using 0.1 M NH_4NO_3 solution (solution to zeolite ratio of 33:1), at 100 °C for 1 h under reflux. It was then washed, dried, and calcined at 500 °C for 6 h under air flow (60 ml $min^{-1}\ g^{-1}$) and the catalyst was named as HY.

2.2. Bottom-up synthesis of hierarchical Y zeolite (ST-HY)

Bottom-up hierarchical Y zeolite was prepared using a modified method described by Tempelman et al. [26]. Briefly, a known quantity of TPOAC organosilane (Si/TPOAC ratio of 45) was added dropwise in the above zeolite precursor solution (i.e., as reported in Section 2.1) and stirred for another 4 h. The resultant mixture was hydrothermally treated at 100 °C for 72 h in a static oven. The solid catalyst was recovered by filtration and subsequently washed with abundant DI water to remove any unreacted zeolite precursor and/or TPOAC. After three successive ion-exchanges using 0.1 M NH_4NO_3 solution (solution to zeolite ratio of 33:1) at 100 °C for 1 h under reflux, followed by drying and calcination at 500 °C for 6 h under air flow (60 ml $min^{-1}\ g^{-1}$), the powdered catalyst was named as ST-HY.

2.3. Top-down synthesis of hierarchical Y zeolite (CT-HY)

The surfactant templating approach was used to prepare a hierarchical Y zeolite using a modified method outlined by Sachse et al. [27]. Prior to modification, NaY zeolite was mildly acid-treated with citric acid monohydrate. To do so, 1 g of NaY was suspended in 6 ml of DI water and stirred magnetically, followed by the dropwise addition of 2 ml of an aqueous solution of citric acid monohydrate (12 wt%) over the course of 1 h. The suspension was filtered and washed with DI water until pH was increased to 7. The dried powder sample was named as NaY-(CA).

In parallel, a solution “A” was prepared by dissolving 0.7 g CTAB in 64 ml aqueous solution of NH_4OH (0.36 M). 1 g of NaY-(CA) was added to solution “A” and stirred for another 1 h at ambient conditions. The mixture was then transferred to a 100 ml PP bottle and hydrothermally treated under static conditions at 90 °C for 12 and/or 24 h. The sample was later recovered by filtration, dried in an oven at 100 °C for 12 h and ion-exchanged (3-times) with 0.1 M NH_4NO_3 as discussed above. Finally, the dried catalyst was calcined under air flow (60 ml $min^{-1}\ g^{-1}$) at 500 °C for 6 h and named using the following nomenclature: CT-HY-1 and CT-HY-2 where 1 and 2 represent two different samples prepared by varying the hydrothermal treatment time of 12 and 24 h, respectively. Fig. S1 illustrates the various steps and system boundary for the synthesis and modification of various zeolite samples. The details regarding the catalytic characterization, catalytic testing and sustainability analysis are presented in the Supporting Information (SI).

3. Results and discussion

3.1. Catalyst characterization

3.1.1. Crystallinity and compositional analysis of the zeolites

Fig. 2a illustrates the PXRD patterns of the parent and hierarchically modified HY zeolite samples within the 2θ range of 5–30°. However, we only compared the peaks with a relative intensity greater than 0.2 %, using the faujasite (FAU) framework peak at 6.2° as the reference (COD 9000124), owing to the presence of small noise in the XRD patterns of the parent and hierarchically modified zeolite samples. Overall, the diffraction peaks of all the samples align with the characteristic peaks of the faujasite (FAU) framework (COD 9000124) at 2θ values of 6.2°, 10.1°, 11.9°, 15.6°, 18.6°, 20.3°, 22.7°, 23.6°, 25.7°, 26.9°, 27.7° and 29.5°, indicating an identical zeolite structure even after the modification [5]. However, the hierarchically modified zeolite samples exhibited a slight peak shift to lower 2θ along with the broadening of peaks as compared to the parent HY zeolite. This could be due to the mild lattice relaxation during reconstruction of zeolite framework, resulting in an increase in d-spacing [34,35]. Similarly, the hierarchically modified zeolite samples showed a reduction in the relative crystallinity compared to that of the microporous HY (Table 1). The reduction of relative crystallinity of hierarchical zeolites might be due to the formation of mesoporosity in the zeolite structure which inherently reduces crystallinity. In detail, the creation of mesopores disrupts the regular repetition of the crystalline structure, resulting in broadening and less pronounced X-ray diffraction patterns [36].

Moreover, Table 1 shows the global Si/Al ratio of the parent and hierarchically modified zeolite samples determined by ICP-OES. All the hierarchical zeolite samples exhibited comparable global Si/Al ratios, suggesting that the hierarchical modification of zeolites did not change significantly their framework composition and functionality. This could be further confirmed by observing the rather similar framework Si/Al ratios of the various zeolite samples, which were estimated based on the unit cell parameter and by applying the Breck-Flanigen equation [37]. Only a small increase in the framework Si/Al ratio is noticed with the degree of hierarchy, which could be associated with the decrease in the number of framework Al as later confirmed by FTIR with pyridine.

3.1.2. Analysis of acid sites in various zeolite samples by infrared spectroscopy

Fig. 2b shows the difference spectra of adsorbed pyridine at 150 °C for the different zeolite samples in the range of 1700–1400 cm^{-1}. All the samples exhibit five broad bands with a difference in their intensities. The two bands at 1455 and 1623 cm^{-1} correspond to the adsorbed pyridine on the Lewis acid sites (PyL) and are associated with the presence of extra-framework Al (EFAl) species. On the other hand, the interaction of pyridine with the Brønsted acid sites (PyH$^+$) results in the

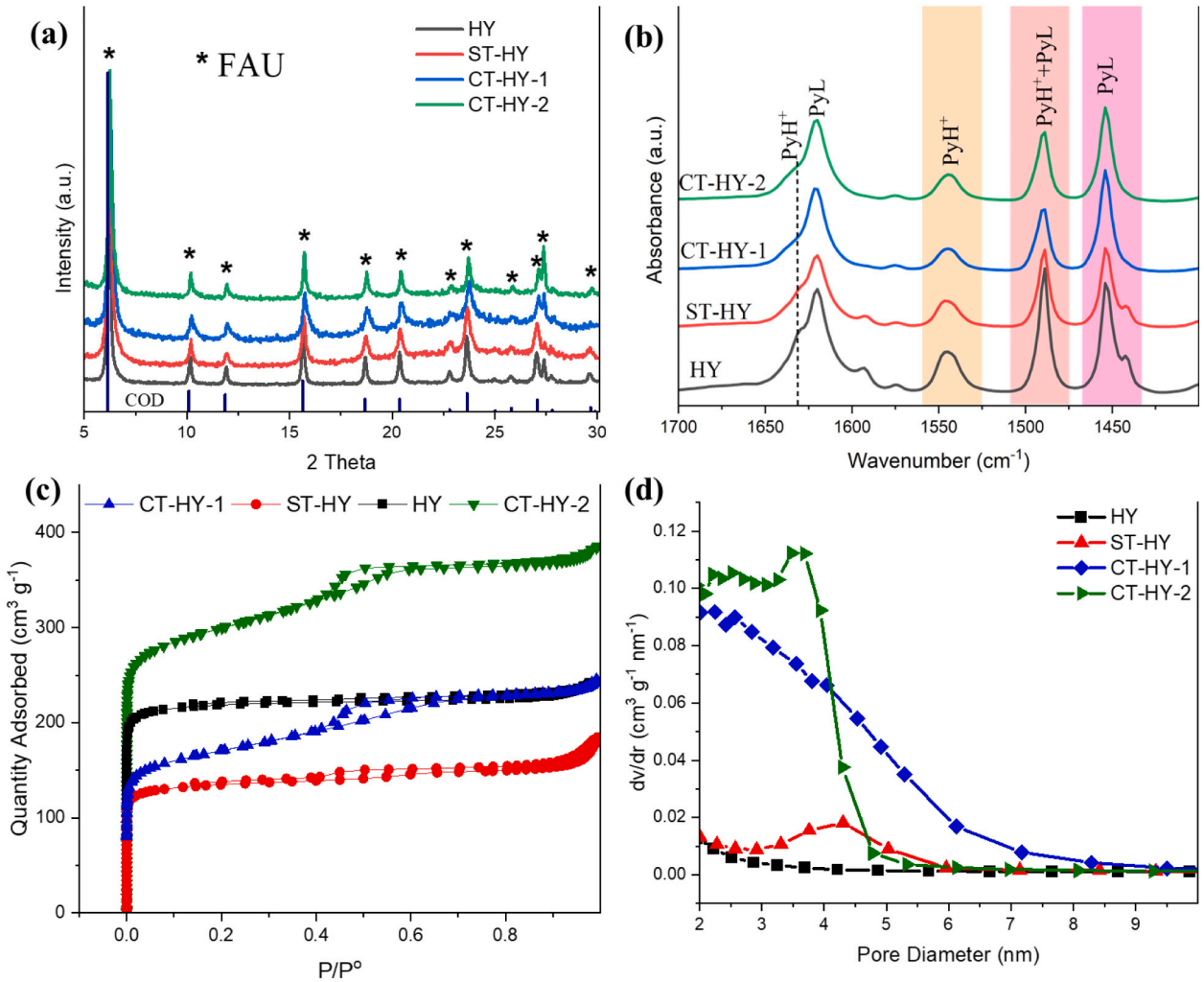

Fig. 2. Physiochemical properties of the parent and hierarchically modified HY zeolite samples: (a) XRD patterns within the 2θ range of 5–30°; (b) FTIR difference spectra after and before pyridine adsorption at 150 °C in the 1700–1400 cm^{-1} range; (c) N_2-physisorption isotherms and (d) BJH adsorption pore size distribution (nm).

Table 1
Physicochemical properties of the various zeolite samples obtained from XRD, ICP,-OES N_2-physisorption, and FTIR-py.

Catalyst	Relative crystallinity	a_o[a]	Si/Al_{IV}[b]	Si/Al[c] (ICP)	V_{micro}	V_{meso}	S_{ext}	S_{BET}	PyH^+	PyL	$\frac{PyH^+_{350°C}}{PyH^+_{150°C}}$	$\frac{PyL_{350°C}}{PyL_{150°C}}$
	%				$cm^3\ g^{-1}$		$m^2\ g^{-1}$		$\mu mol\ g^{-1}$		%	%
HY	100	24.585	3.23	2.13	0.299	0.070	90	650	520	571	6	25
ST-HY	85	24.532	3.89	2.14	0.152	0.103	141	431	342	408	11	32
CT-HY-1	79	24.518	4.10	2.44	0.148	0.218	270	531	279	472	11	43
CT-HY-2	71	24.524	4.00	2.44	0.297	0.286	390	913	322	432	16	47

[a] Unit cell parameter calculated from XRD.
[b] Framework Si/Al calculated from the unit cell parameter using the Breck-Flanigen equation [37].
[c] Global Si/Al determined from elemental analysis (ICP-OES).

appearance of two bands at 1547 and 1640 cm^{-1}. Moreover, a distinct band at 1490 cm^{-1} shows the simultaneous interaction of pyridine with both Brønsted and Lewis acid sites. Finally, the small bands at 1575–1585 cm^{-1} are associated with co-ordinately bonded pyridine at Lewis acid sites [38]. However, these bands are less prominent in hierarchical zeolite samples due to their lower Lewis acid sites as compared to HY (Table 1).

Furthermore, Table 1 presents the acidic properties of the various zeolite samples. The parent HY zeolite showed the highest concentration of Brønsted and Lewis acid sites, which are associated with the presence of framework Al (FAl) and EFAl species respectively. On the other hand, the bottom-up approach (ST-HY) and top-down modification of zeolites show a reduction in the Brønsted and Lewis acid sites, which might be due to slight removal of FAl and EFAl species during the hierarchical modification. In comparison to CT-HY-1, the slightly higher number of Brønsted acid sites for CT-HY-2 could be due to the highest pore volume, as observed in Section 3.1.3, which may have led to improved pyridine accessibility to the Brønsted acid sites. This is not surprising considering the removal of a higher amount of EFAl species in CT-HY-2 (i.e., lower Lewis acidity).

Table 1 also shows the acidic strength of Brønsted and Lewis acid sites for the parent and hierarchically modified zeolite samples by comparing the number of acid sites able to retain pyridine at 150 and 350 °C. All hierarchically-modified zeolite samples displayed slightly higher Brønsted acid sites strength than the parent HY, which may be associate with the decrease in the density of the Brønsted acid sites which is accompanied by a slight increase in the framework Si/Al. Similar results were observed for the Lewis acidic strength of the different samples, where all the modified samples showed higher Lewis acidic strength as compared to the parent HY, with the increase in the strength of Lewis acid sites being much more significant than for Brønsted acid sites. Overall, acid strength linearly increased with an increase in textural properties of hierarchical zeolites (Section 3.1.3), suggesting that an increase in mesoporosity provides better accessibility to inherently stronger internal acid sites [39].

3.1.3. *Textural properties of the different zeolites*

Fig. 2c shows the nitrogen isotherms of the parent and hierarchically modified zeolite samples. All the samples exhibit distinct hysteresis loops and quantities of nitrogen adsorbed, confirming a change in the textural properties of the zeolite samples during the treatment. Overall, the parent HY zeolite exhibited type I isotherm, confirming the presence of microporous structure [26]. On the other hand, ST-HY showed a combination of type I + II isotherm, suggesting the formation of mesoporosity [40,41]. Similarly, top-down hierarchically modified zeolite samples showed a combination of type I and IV isotherm with a sharp nitrogen uptake at relative pressure of $P/P^0 = 0.4–0.6$, indicating the presence of uniform mesoporosity [27,42]. Overall, the isotherms ended with nearly horizontal plateau at high relative pressure, indicating that all hierarchical zeolite samples have no large mesopores/macropores as confirmed by pore size distribution. Furthermore, BJH adsorption curves of the various zeolite samples (Fig. 2d) also show the presence of mesopores within the range of 2–10 nm for all samples, with the top-down hierarchically modified zeolites presenting more developed mesoporosity. However, CT-HY-1 resulted in broader and occasionally larger mesopores with lower density as compared to CT-HY-2. This could be due to the incomplete micelle formation during the treatment time. In contrast, CT-HY-2 with the maximum mesopore volume showed relatively smaller average pore diameter with the maximum pore density, suggesting the formation of uniform and packed micelle formation during the prolonged synthesis time [8,43]. Fig. S2 compares the nitrogen isotherm of HY and citric acid modified zeolite samples. The citric acid treated zeolite showed identical isotherm to that of the parent Y zeolite, confirming that the mild acid treatment only leads to minor changes to the textural properties as later discussed.

To quantify this, Tables 1 and S4 compare the textural characteristics of the parent and modified zeolite samples. As expected, HY displayed the usual characteristics of a microporous zeolite with high microporous volume and relatively low mesoporosity. On the other hand, ST-HY zeolite showed an increase in mesoporous volume (+47 %) and external surface area (+57 %), confirming the generation of mesopores due to the entrapment of organosilane template during the crystallization step and its subsequent removal after calcination. However, the sample showed a much lower adsorption of N_2 at very low pressure (Fig. 2b), attributing to a significant decrease in the micropore volume (−49 %) caused by the detrimental effect of the formation of mesoporosity on the micropore volume (i.e., constricted mesoporosity) [44]. In the case of the CT-HY samples, the pre-treatment of the Y zeolite with citric acid led to a slightly improvement of the micropore volume (Table S4), pointing to a slight dealumination of the parent Y zeolite. However, it resulted in a decrease in the mesopore volume and external surface area. Citric acid pre-treatment is important as it opens the Si-O-Al bonds and creates enough surface defects required to add large mesoporosity during the top-down modification. As a result, the top-down templating treatment of the acid-treated Y zeolite resulted in a general substantial improvement in the textural properties. Overall, CT-HY-1 exhibited a much larger mesopore volume (+211 %) and external surface area (+200 %) than the parent Y zeolite, confirming the diffusion of CTA^+ molecules from the solution to the pores of the zeolite. As suggested by Sachse et al., [27] the diffusion is caused by the attraction of Si—O sites formed by the base and, once inside, CTA^+ molecules self-assemble into micelles, thereby causing the meso-structuring of the zeolite crystals after calcination [45]. Despite this, it led to a notable decrease in the micropore volume of the resultant zeolite which might be due to the following reasons: (i) the presence of EFAl as debris around the partially packed micelles, as previously observed by slightly higher Lewis acidity as compared to CT-HY-2, (ii) incomplete surfactant-templating process [27]. This could be confirmed by extending the treatment time to 24 h. In fact, CT-HY-2 showed the highest mesopore volume (+309 %) and external surface area (+334 %), suggesting the completion of the surfactant templating process. This could be further confirmed by observing the restoration of the micropore volume (i.e., similar to that of HY), which may have resulted from the completion of the surfactant templating process and/or structural reorganisation

owing to the extended treatment time [43]. Similarly, it might be due to the formation of surface defects without the collapse of the zeolite structure. However, the significant increase in textural properties might have been accompanied by a small dissolution of the silica as observed by the decrease in the crystallinity of this sample and also according to previous literature [27].

4. Catalytic experiments for the hydrocracking of HDPE

4.1. Conversion and overall product distribution

Fig. 3a illustrates the results of the catalytic hydrocracking of virgin HDPE conducted at 325 °C for 1 h under 30 bar cold H_2 pressure. Overall, the HY zeolite showed the least conversion (19.4 %) among the tested zeolites. The low conversion of HDPE showed that the surface acidity of the parent HY zeolite is not sufficient to crack the long-chain polymers into short-chain intermediates, suitable for diffusion into the micropores of zeolite. Similarly, despite having the maximum number of acid sites (1091 μmol g^{-1}), the microporous HY zeolite did not provide sufficient access to bulkier polymeric chains, leading to suboptimal catalyst utilization and reduced conversion. To mitigate these issues, various hierarchical HY zeolite samples with distinct textural and comparable acidic properties were tested. Interestingly, all hierarchical HY zeolite samples showed an increase in the overall conversion (Fig. 3a). The overall increase in the conversion of the zeolites follows the order: HY (19.4 %) < ST-HY (21.6 %) < < CT-HY-2 (33.3 %) < CT-HY-1 (35.1 %). To unlock the effects of different physiochemical properties (i.e., porosity, surface area, acidity and acidic strength) of each zeolite sample on the conversion, we proposed the reaction mechanism for the hydrocracking of linear chain HDPE over the zeolite shown in Fig. 3b. Briefly, the reaction initiates with the adsorption of the molten polymer on the external surface of zeolite, followed by classical β-scission mechanism. Therefore, the hierarchical HY zeolites with high external surface area provide more surface sites for bond scission, leading to the formation of shorter-chain polymers (i.e., initial carbenium ions). Similarly, the enhanced mesopore volume of the hierarchical HY zeolites led to easy penetration of the carbocations into the pores where the maximum acid sites are present, resulting in the formation of small carbocations and olefins. Finally, the olefins undergo hydrogenation owing to the presence of high partial pressure of hydrogen before being emerged into the end product. Therefore, this generally demonstrates the progressive increase in conversion as a function of the improved external surface area and mesoporous volume. Indeed, considering the significant decrease in Brønsted and Lewis acidity for the hierarchical zeolites as opposed to the parent HY, higher positive changes in mesoporous volume and external surface area seem to be one of the main drivers for the increase in conversion, as a result of the better accessibility of polymer chains to the acid sites. Besides textural properties, and despite the fact that the overall number of acid sites on the hierarchical zeolites is smaller than for the parent HY zeolite, the conversion also appears to increase with the increase in ratio of Lewis acid sites/Brønsted acid sites (L/B), with CT-HY-1 (L/B = 1.69) showing the maximum ratio followed by CT-HY-2 (L/B = 1.34) and ST-HY (L/B = 1.19), whereas HY exhibited the least ratio (L/B = 1.10). This is in accordance with the previous literature, where Pyra et al. [46] suggested the dominant role of Lewis acid sites towards the initiation of the plastic hydrocracking. As such, the presence of Lewis acid sites promotes the cracking via hydride abstraction, resulting in the formation of carbenium ions for subsequent reactions. However, it is also important to retain the Brønsted acid sites (BAS), which leads to the cracking of the formed carbenium ions into small carbocations and olefins. Therefore, a balance between Lewis and Brønsted acid sites controls the reaction pathways, with the higher activity over catalysts with a high L/B ratio. In addition, the fact that the CT-HY-2 and CT-HY-1 zeolites present similar levels of conversion may suggest that a further increase in textural properties of CT-HY-2 does not significantly influence the activity of the zeolites for the hydrocracking of plastics, when the other physicochemical parameters remain similar. This could be further supported by previous literature [6,17]. Based on the conversion results, we developed an empirical correlation which collectively assesses the impact of different physiochemical properties of each zeolite sample on the conversion and named it the conversion factor [47,48].

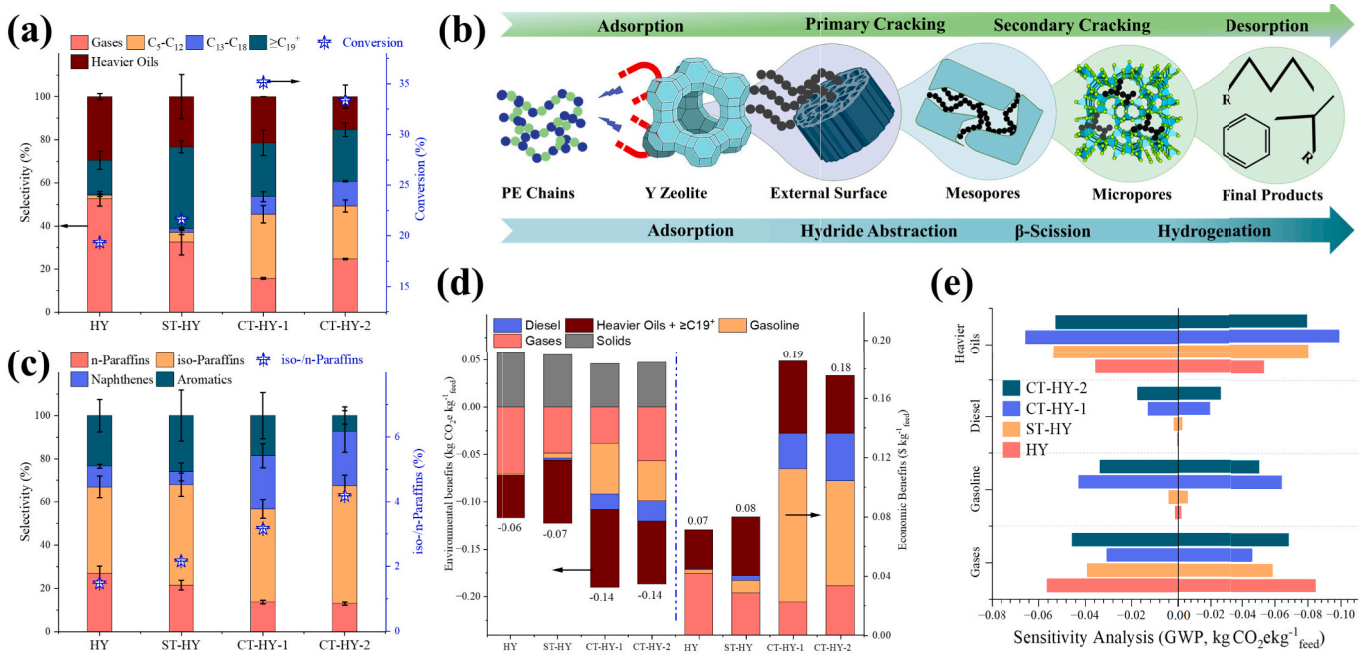

Fig. 3. (a) Performance comparison and product distribution of hydrocracking of HDPE over different catalysts; (b) proposed reaction mechanism of hydrocracking HDPE over zeolites; (c) product composition of gasoline range hydrocarbons over various zeolites; (d) comparison of various zeolite samples based on their positive impact on environment (GWP CO_2e kg^{-1}_{feed}) and economic benefits ($ kg^{-1}_{feed}), and (e) sensitivity analysis in terms of environmental benefits for different value-added products obtained during the hydrocracking of HDPE over various zeolite samples.

This was done by evaluating the individual role of each physiochemical property on the hydrocracking reaction mechanism and is discussed in detail elsewhere in the literature [5]. A detailed discussion is part of SI.

Moreover, in terms of product distribution, HY exhibited the maximum selectivity of gases (52.6 %) and heavier oils (29.5 %). This suggests that the hydrocracking reaction over microporous HY zeolite dominantly occurred by an end-of-chain cracking mechanism [24,49], resulting in high selectivity of gases (i.e., C_1-C_4). Similarly, the long-chain intermediates formed after the initial cracking were unable to diffuse into the small pores where the maximum number of active sites are located. As a result, the reaction ended up with the hydrogenation of long chain olefins into heavier oils, and with low selectivity of lighter oils (17.9 %), especially C_5-C_{18} (2 %). In comparison to the parent HY zeolite, ST-HY showed slightly better selectivity of lighter oils (44.2 %) at the expense of gaseous products (32.5 %) and heavier oils (23.3 %). This suggests that the increase in mesoporosity and external surface area improve the diffusion of heavier oils into the pores of the zeolites. Despite this, ST-HY insignificantly enhances the selectivity of middle distillates (C_5-C_{18} = 6.3 %), owing to a slight increase in acid strength. In contrast, both CT-HY samples exhibited high selectivity of lighter oils (60–62.8 %) at the expense of heavier oils (~15–21 %), confirming the significance of an enhanced mesoporosity that provides higher accessibility to the active sites and of the higher acidity strength for the extent of cracking. As a result, both top-down hierarchically modified zeolite samples displayed the maximum products within the C_5-C_{18} range (36–38 %).

Moreover, Fig. 3c shows the product composition of gasoline-range hydrocarbons over the various zeolite samples. Overall, all the samples showed maximum affinity towards paraffins as compared to naphthenes and aromatics, with a higher proportion of iso-paraffins in the product as compared to n-paraffins, as expected according to the hydrocracking mechanism [50]. In comparison to HY, all the hierarchical HY zeolite samples showed an increase in the iso−/n-paraffin ratio, as the improved mesoporosity can facilitate the diffusion of the more ramified molecules out of the zeolite structure. As a result, CT-HY-2 with the maximum pores volume and external surface area exhibited the highest iso-/n-paraffin ratio of 4.2. Similarly, the lower retention time of molecules in the hierarchical zeolites structure may have led to the decrease in the preponderance of aromatisation reactions, significantly reducing the selectivity of aromatics. Despite this, both CT-HY samples displayed significantly high selectivity of naphthenes (24–25 %) as compared to ST-HY (6 %). This could be due to the higher reaction rates observed over CT-HY samples and/or to the increase in the significance of cyclization reactions involving bulkier reaction intermediates due to the increase in the space within the zeolite structure [5,51].

Finally, Fig. 3d presents the sustainability assessment of the various zeolite samples based on the positive impact of their valuable products (i.e., avoided products) in terms of their global warming potentials (kg CO_2e kg_{feed}^{-1}) and economic cost (\$ kg_{feed}^{-1}). The methodology is part of SI. As expected, the HY zeolite displayed the least environmental (−0.06 kg CO_2e kg_{feed}^{-1}) and economic benefits (0.07 \$ kg_{feed}^{-1}), due to its lower conversion of HDPE. Similar results were observed over ST-HY where the catalyst marginally improved the environmental and economic benefits of the process. However, both top-down hierarchically modified HY zeolite samples showed a significant and comparable increase in the environmental and economic benefits, confirming the benefits of top-down modified hierarchical mesopores zeolites towards the hydrocracking of HDPE. This is further supported by the sensitivity analysis in terms of environmental benefits of value-added products obtained over different zeolite samples (Fig. 3e). Overall, HY exhibited the maximum sensitivity towards low-value gaseous products in relation to the change of individual parameter (i.e., ±20 % in the yield of each valuables). Similarly, ST-HY showed the high sensitivity towards gases and heavier hydrocarbons. However, both HY and ST-HY displayed negligible sensitivity towards gasoline and diesel range hydrocarbons. In contrast, both top-down hierarchically modified zeolite samples led to improve the sensitivity of gasoline and diesel range hydrocarbons, suggesting a high potential for environmental benefits, owing to the diverse product distribution at lower reaction temperature.

To conclude, hierarchical zeolite samples showed high conversion of HDPE as compared to conventional HY. In line with this, CT-HY samples exhibited the highest conversion with the maximum selectivity of lighter oils within gasoline and diesel range hydrocarbons, owing to the presence of significant mesopores and high L/B ratio. An additional increase in the external surface area and mesopores volume as observed for CT-HY-2, however, does not seem to further enhance the activity of the zeolite. Compared to microporous HY and ST-HY, top-down hierarchically modified zeolite samples also showed higher iso-/n-paraffins and lower aromatics formation, with the maximum and minimum values, respectively, being achieved over CT-HY-2 owing to its higher textural parameters. It can be, therefore, concluded for zeolites with similar number of acid sites that while the conversion of plastics is not altered once a threshold in mesoporosity is reached, a further increase in the mesoporous volume can have a greater impact on the quality of the gasoline range hydrocarbons produced. In terms of sustainability analysis, CT-HY zeolite samples showed the maximum and comparable environmental and economic benefits due to their high catalytic activity.

4.2. Effect of reaction temperature and process optimisation

The catalytic hydrocracking of plastics has been showing better conversion and activity results towards lighter oils (i.e., gasoline and diesel range hydrocarbons) as compared to conventional chemical recycling methods [52–54]. However, the advantages of the process are directly related to the properties of the employed catalysts and the intrinsic reaction conditions (i.e., temperature and reaction time). For instance, an increase in reaction temperature leads to improvements in the cracking rates and the overall conversion. However, it resulted in a significant shift in the product distribution from lighter oils to gaseous products due to the occurrence of secondary cracking reactions. As a result, the environmental and economic benefits of various zeolite samples at higher reaction temperatures are primarily influenced by the selectivity of the resultant products (i.e., gases, lighter oils, and heavier oils) rather than by the difference in their conversions. Therefore, the optimisation of the catalytic hydrocracking of HDPE over various zeolite samples and at different reaction temperatures (325–390 °C) was done using the Pareto front optimisation approach. The detailed methodology is provided in (SI). Briefly, the catalytic results considering conversion and environmental and economic analyses of the valuable products at distinct reaction temperatures were normalised and compared to conclude on the most optimized reaction temperature. However, to keep the calculations simple, the energy depletion at each reaction temperature was considered a controlled variable, as all the catalysts at distinct reaction temperatures consumed the same energy.

Fig. 4a illustrates the results of catalytic hydrocracking of HDPE over the various zeolite samples at different reaction temperatures. Overall, an increase in reaction temperature resulted in an increase in the conversion, and all the samples eventually exhibited comparable conversion results (94–99 %) at 390 °C. This suggests that the high temperature led to surpass the activation energy barrier that affected the activity of the different zeolites at lower temperatures (i.e., 325–360 °C). As a result, all the samples displayed a decrease in the affinity of heavier oils with an increase in temperature from 325 to 390 °C. Contrary to this, the selectivity of lighter oils reached a plateau at 360 °C and later decreased at 390 °C, which is due to the over-cracking of lighter oils into gaseous products, as confirmed by the increase in the selectivity of gases at 390 °C as compared to the results at 360 °C. Interestingly, at 390 °C, while conversions are identical for all zeolites, they present distinct product selectivity, suggesting the significant impact of the textural and acidic properties on the distribution of products. Briefly, HY showed a

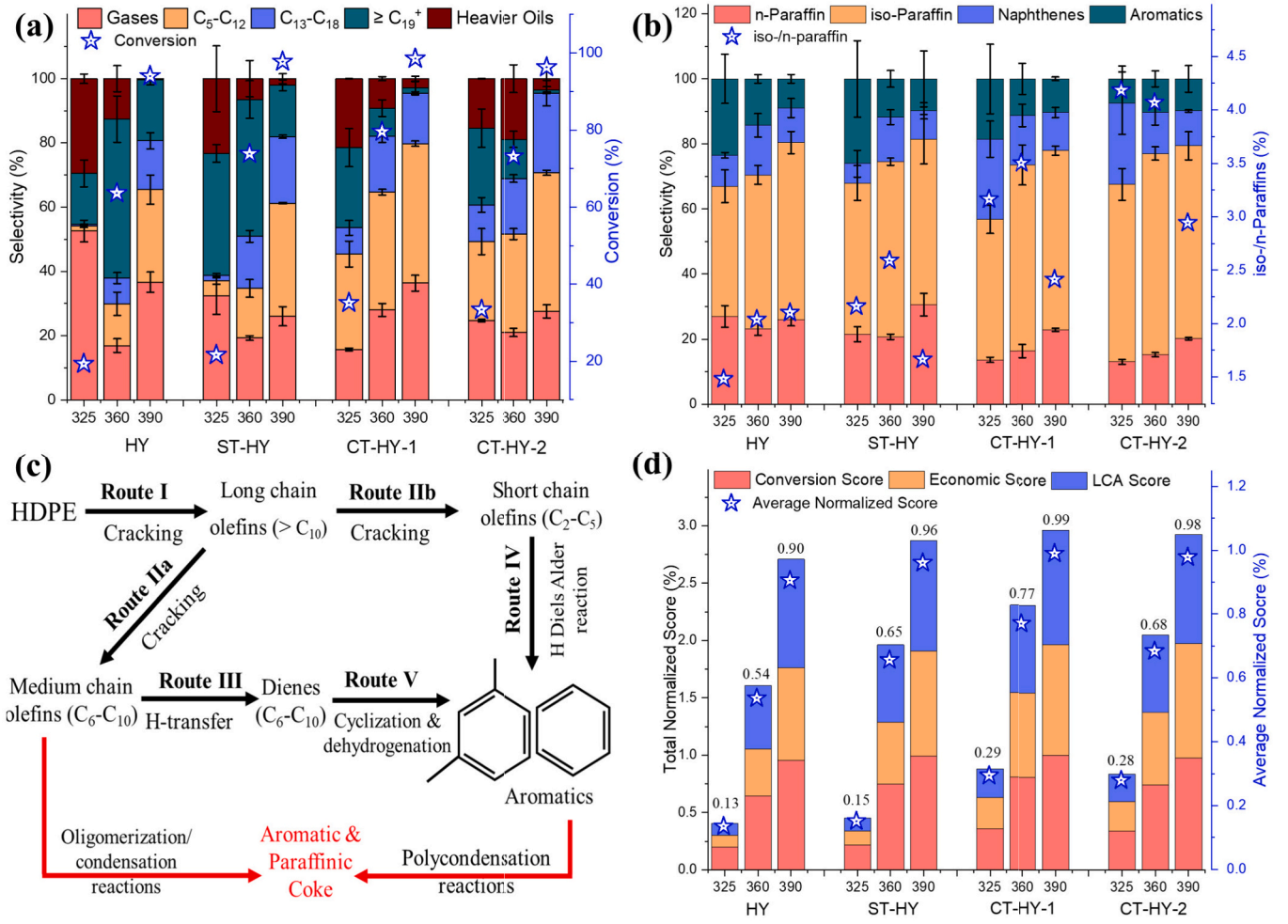

Fig. 4. (a) Performance comparison and product distribution of various zeolite samples at different reaction temperatures; (b) product composition of gasoline range hydrocarbons over various zeolite samples at different reaction temperatures; (c) simplified reaction mechanism for the formation of paraffinic and aromatic coke during the hydrocracking of HDPE at high reaction temperature; and (d) pareto front optimisation of conversion, and environmental (LCA) and economic benefits score achieved over various zeolite samples at different reaction temperatures.

high affinity towards ≥C19$^+$ (~19 %) at 390 °C followed by ST-HY (15.9 %), whereas both CT-HY exhibited the least affinity (0.9–1.7 %). In contrast, both top-down hierarchically modified zeolites exhibited high selectivity towards middle distillates (C_5-C_{18}), with the maximum value achieved over CT-HY-2 at 390 °C (67.9 %).

Moreover, Fig. 4b compares the product composition of gasoline range hydrocarbons over the various zeolite samples at different reaction temperatures. Overall, with an increase in reaction temperature, HY showed an increase in the iso-/n-paraffin ratios, whereas all the hierarchical HY zeolite samples displayed a decrease in the ratio of iso-/n-paraffins. This could be due to the improved reaction rates over the hierarchical zeolite samples which may favour the secondary cracking of isomerised species at elevated temperature. Similarly, with an increase in reaction temperature, both HY and ST-HY showed a decrease in the selectivity of aromatics whereas the selectivity of naphthenes remained the same. Contrary to this, top-down hierarchically modified zeolite samples showed a significant decrease in the selectivity of naphthenes, whereas the selectivity of aromatics showed minimal variation. The decrease in the selectivity of naphthenes and aromatics suggested the occurrence of side-reactions leading towards coke formation. To understand this uncommon trend, we performed the TGA analysis of various spent catalysts at 390 °C (Fig. S5a–b). Interestingly, both CT-HY zeolite samples showed the presence of significantly high paraffinic (40–45 wt%) and aromatic coke content (17–18 wt%) [6,55]. The high coke content over less acidic catalysts (i.e., top-down hierarchically modified zeolites) strengthens our previous argument that, despite being less acidic, the improved textural properties of both top-down hierarchically modified zeolites provided better accessibility to acidic sites as compared to the microporous HY zeolite. Furthermore, based on the results, we proposed a reaction mechanism for the coke formation over the zeolites as illustrated in Fig. 4c. Overall, at high reaction temperatures, the long HDPE chain undergoes β-scission, resulting in the formation of long-chain olefins (route I) [56]. The long-chain olefins further cracked medium-chain olefins (route IIa) and short-chain olefins (route IIb) owing to the high reaction temperature. These medium chain olefins (C_6-C_{10}) were converted through H-transfer to dienes (route III), which subsequently formed monoaromatics through cyclization and dehydrogenation (route V). Alternatively, the medium chain olefins (C_6-C_{10}) may undergo side reactions (i.e., oligomerization and condensation reactions) to form paraffinic coke. Similarly, the short-chain olefins (route IV) form mono-aromatics (BTX), which subsequently form poly-aromatics (i.e., aromatic coke) via polycondensation reactions [57]. Therefore, the high paraffinic and aromatic coke over top-down hierarchically modified zeolites suggested the improved textural properties led to improve the diffusion of bulkier molecules into the pores, where the rapid cracking and occurrence of several side reactions resulted towards coke formation. This is also consistent with the higher space available inside the structure of hierarchical zeolites for bulkier

transitions and intermediates leading to coke formation.

Furthermore, Fig. S5c illustrates the DTG curves for the oxidation of different types of coke over various zeolite samples. Briefly, HY shows a prominent peak at 275 °C, suggesting the presence of soft coke. In contrast, top-down hierarchical zeolite samples exhibited intense peaks at relatively high temperatures (345–390 °C), indicating the presence of soft coke within the mesopores of the zeolite [58]. A similar trend was observed in the aromatic coke region, where both HY and ST-HY exhibited peaks at relatively lower temperatures (500–520 °C), whereas top-down hierarchically modified zeolite samples showed a prominent peak at 535 °C, suggesting a higher content of hard coke (i.e., acidic coke) in CT-HY samples owing to their high acidic strength [59]. To validate this, we compared the coke content over HY (minimum activity) and CT-HY-1 (maximum activity) at different reaction temperatures (i.e., 325–390 °C). At low reaction temperature (325 °C), HY exhibited a broader peak at 420–450 °C, which significantly reduced and shifted to low temperature range at high reaction temperatures. In contrast, CT-HY-1 showed the peak shifting to high temperatures at higher hydrocracking reaction temperature (360 °C–390 °C), suggesting the occurrence of side reaction which led to produce paraffinic coke. Similar trend was observed in the aromatic coke region over CT-HY-1 sample. To observe the effect of coke content on the textural properties of zeolite samples, we regenerated the recovered catalysts at 500 °C and studied their textural properties (Table S6). Briefly, all the samples exhibited a significant decrease in the micropore volume, owing to the presence of aromatic coke as observed by the TGA and DTG analysis (Fig. S5). Interestingly, HY showed a complete regeneration of the mesoporous volume and 85.6 % regeneration of the external surface, confirming the ease in oxidation of coke as discussed above. On the other hand, the partial regeneration of the textural properties of the hierarchical zeolite samples suggested the requirement of high-temperature regeneration for the complete removal of coke species. Despite this, both top-down hierarchically modified zeolite samples showed higher textural properties, mesopore volume, and external surface area than the parent HY zeolite. Similarly, Fig. S5e compared the performance of HY and CT-HY-1 before and after regeneration at 325 °C. Briefly, HY-$_{regenerated}$ showed only 15 % conversion, whereas CT-HY-1-$_{regenerated}$ exhibited a conversion of 24 %. A slightly lower conversion for both HY-$_{regenerated}$ and CT-HY-1-$_{regenerated}$ as compared to their fresh counterparts suggests an incomplete regeneration of the catalysts at 500 °C. In terms of product distribution, both regenerated zeolites showed high selectivity of gases with a decrease in the selectivity of heavier oils as compared to their fresh counterparts. This could be due to the incomplete pore opening of both zeolites after regeneration, thereby favouring cracking mainly on the external surface of zeolite. Despite this, CT-HY-1-$_{regenerated}$ showed 1.6-times higher conversion as compared to HY-$_{regenerated}$, confirming the significance of hierarchical structure for the improved conversion of HDPE.

Furthermore, Fig. S5f demonstrated the environmental benefits of the obtained products (i.e., avoided products) over the various Y zeolite samples at different reaction temperatures. As expected, an increase in reaction temperatures improved the environmental benefits, with the maximum positive impact at 390 °C for all zeolite samples. This could be due to an increase in the overall conversion (i.e., decrease in solids). Briefly, CT-HY-1 showed the most benefits at each reaction temperature, owing to the maximum catalytic activity of the sample. Similarly, both ST-HY and CT-HY-2 displayed similar results at higher reaction temperatures (360–390 °C), whereas HY matched the impact values of ST-HY and CT-HY-2 at 390 °C. On the other hand, Fig. S5g compares the catalytic activity based on the economic benefits of the resultant products at each reaction temperature. Similar results were observed where an increase in reaction temperatures improved the economic benefits due to an increase in conversion. However, some variations in the economic results were observed, suggesting that the change in product distribution over temperature changes the overall economic score. For instance, CT-HY-2 showed the maximum economic benefits at 390 °C, owing to the maximum selectivity of lighter oils (67.9 %). Despite having similar conversion values, HY and ST-HY samples displayed a significant variation in the economic benefits as a result of distinct product distribution. Therefore, Pareto front optimisation was performed to simultaneously compare the results of the various catalysts based on their conversion, environmental and economic benefits. Fig. 4c shows the Pareto front normalised score of the various catalysts at different reaction temperatures. The detailed discussion is part of SI (Table S5 and Fig. S4). At each reaction temperature, CT-HY-1 showed the maximum total and average normalisation score closely followed by CT-HY-2 and ST-HY, whereas the parent zeolite displayed the minimum values, suggesting that the CT-HY-1 is the best performing catalyst for the hydrocracking of HDPE.

To conclude, an increase in reaction temperature significantly increases the conversion and selectivity of lighter oils over the zeolite samples. However, at the same conversion level, the product distribution is a function of the catalytic physiochemical properties of each zeolite. Both HY and ST-HY showed more affinity towards $\geq C19^{+}$, whereas CT-HY mesoporous zeolites exhibited high selectivity of middle distillates. Also, an increase in reaction temperature led to an improvement in the iso-/n-paraffin over HY, whereas all hierarchical zeolite samples showed a decreasing trend. Moreover, top-down hierarchical zeolite samples are prone to deactivation and need high-temperature regeneration, owing to the deposition of a significant amount of coke. Despite this, CT-HY-1 showed higher conversion as compared to HY after regeneration. The sustainability assessment of product distribution showed that the high selectivity of lighter oils (C_5-C_{18}) range hydrocarbons significantly improved the environmental and economic benefits of the catalyst. Finally, the Pareto front optimisation suggests that CT-HY-1 is the best-performing catalyst in terms of catalytic conversion and obtained product distribution.

4.3. Insight into the hydrocracking of real-world plastic waste

All the zeolite samples were further compared towards the hydrocracking of real-world mixed plastic waste at 350 °C for 1 h under 30 bar cold H_2 pressure. The experimental temperature was considered based on the theoretically calculated degradation temperature of mixed post-consumer plastic waste. At 350 °C, only 5 % of the mixed plastic waste was degraded under inert atmosphere (Fig. S6b), suggesting that the temperature is reasonable to compare the hydrocracking results. Similarly, the TGA analysis confirmed the ease in the degradation of PP, PS, and LDPE as compared to HDPE (Fig. S6). This is due to the high crystallinity and presence of strong intermolecular forces in HDPE as compared to other polymers, resulting in a resistance to its cracking.

Based on the results (Fig. 5a), CT-HY-2 showed the maximum conversion (77.3 %), followed by CT-HY-1 (69.4 %) and ST-HY (64.2 %), whereas the parent HY zeolite showed the least conversion (61.9 %). Herein, the maximum conversion over CT-HY-2 showed the prominent role of the improved textural properties of this zeolite for the cracking of mixed plastic waste and, especially branched-chain polymers (i.e., LDPE and PP), as opposed to what had been observed previously during the hydrocracking of unbranched-chain virgin HDPE. Similar results were reported by Jumah et al. [60] and Li et al. [32], who compared the hydrocracking of virgin and post-consumer plastic waste and reported lower activity over branched-chain polymers as compared to straight-chain plastics (i.e., HDPE). In fact, this might be due to the high effective cross-sectional diameters of PP, PS and LDPE oligomers as compared to HDPE, which caused an increase in diffusional limitations during the hydrocracking process [7,60]. This shows that despite the ease to initiate the degradation of LDPE, PS, and PP as compared to HDPE, the hydrocracking results are dependent on the textural properties of the zeolite [6].

This could be further confirmed by performing TGA analysis to the solid residue (i.e., unreacted polymer and catalyst) obtained after the hydrocracking reaction (Fig. S7a). As expected, CT-HY-2 exhibited the

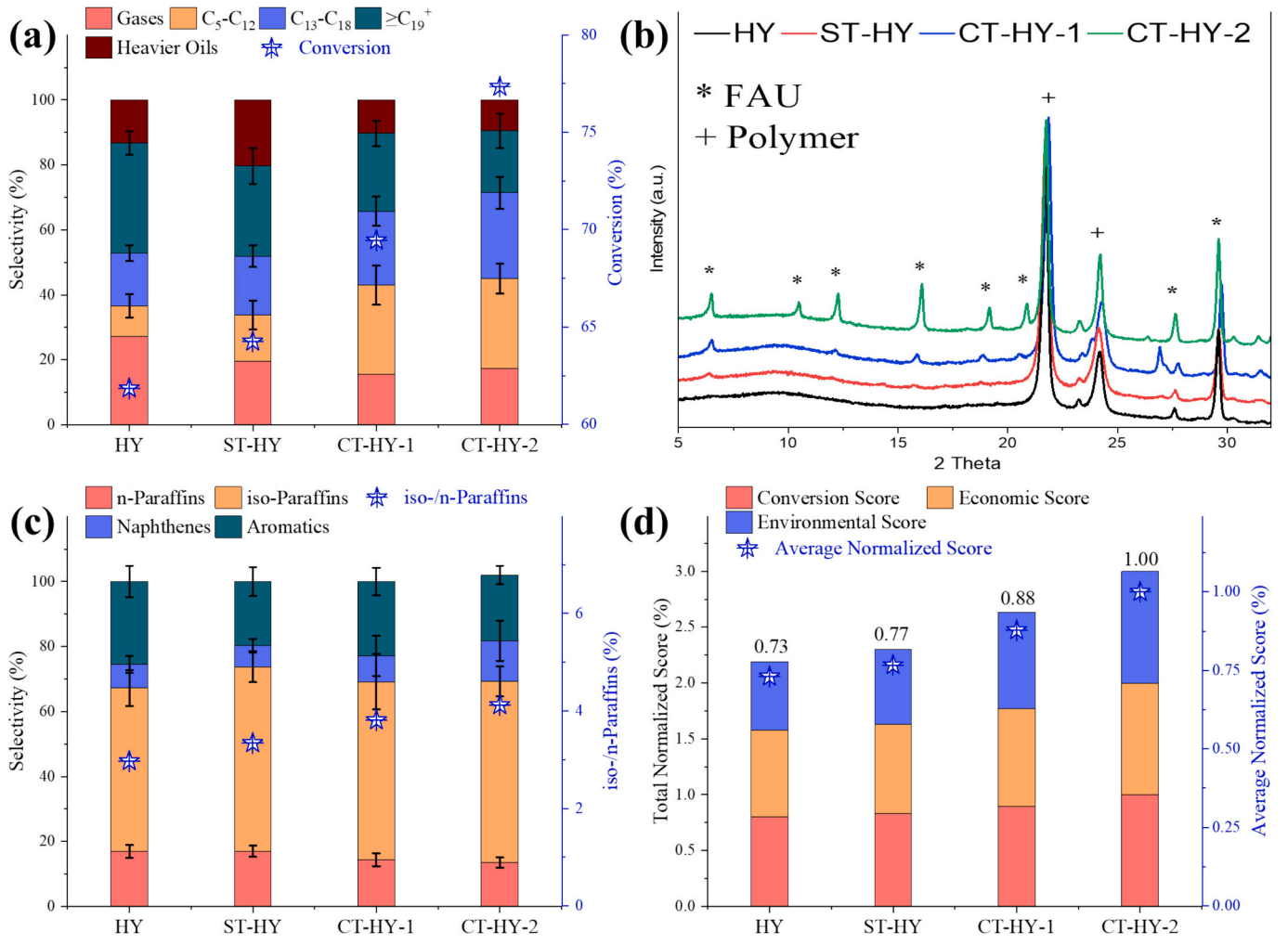

Fig. 5. (a) Performance comparison and product distribution of various zeolite samples; (b) XRD analysis of spent zeolite samples; (c) product composition of gasoline range hydrocarbons over various zeolite samples; and (d) pareto front optimisation of conversion, and environmental and economic benefits score achieved over various zeolite samples.

smallest weight loss, followed by CT-HY-1, whereas both ST-HY and HY showed the maximum weight loss. This confirmed the presence of a minimum amount of unreacted polymer over the surface and/or within the pores of CT-HY-2 as compared to other zeolite samples. Despite this, CT-HY-2 showed the maximum content of aromatic coke (37.7 wt%) followed by CT-HY-1 (27.3 wt%), whereas both ST-HY and HY displayed comparable aromatic coke content (~24–25 wt%), suggesting the formation rate of aromatic coke is linearly dependent on the conversion [61]. To further evaluate the unreacted polymer type, Fig. S7b illustrates the DTG curves of the various solid residues obtained after the hydrocracking reaction as a function of temperature. The DTG decomposition curves were qualitatively compared with the DTG curves of post-consumer plastic waste samples (Fig. S7c). Interestingly, all the samples showed a distinct peak at ~470 °C, suggesting the presence of unreacted post-consumer HDPE. However, HY, ST-HY, and CT-HY-1 showed some other peaks at 340–360 °C, attributed to the oligomers of PP/LDPE. This suggests that the branched-chain polymers were initially cracked on the external surface of zeolite, but some of the formed oligomers were unable to diffuse into the pores of the zeolites. This observation was further supported by the XRD analysis of the spent catalysts as shown in Fig. 5b. All zeolite samples showed significant amorphization due to the deposition and/or presence of unreacted polymer over the surface of the catalyst. As a result, HY and ST-HY mostly showed broad amorphous bands and bands consistent with the presence of unreacted polymer, whereas CT-HY-1 exhibited small peaks corresponding to the crystalline FAU. In contrast, CT-HY-2 displayed more prominent crystalline peaks, suggesting that its improved textural properties led to an enhancement in the hydrocracking reaction with smaller deposition of unreacted polymer over the surface. Moreover, in comparison to HY, all the hierarchical zeolite samples exhibited the aromatic coke peak at slightly higher temperature, with the maximum temperature for CT-HY-2 (Fig. S7b), suggesting the formation of hard coke over hierarchical zeolites as discussed earlier. To observe the effect of aromatic coke content on the textural properties of zeolites, we performed the nitrogen physisorption of the least (HY) and best performing catalysts (CT-HY-2), and the results are illustrated in Table S7. As expected, both samples exhibited a decrease in the textural properties, owing to the presence of aromatic coke. However, in opposite to what has been observed previously for the regenerated samples from the hydrocracking experiments at 390 °C, HY displayed a significant decrease in the mesopore volume and external surface area, whereas CT-HY-2 showed a relatively lower reduction in textural properties. This might be due to the difference in the feedstock as mixed plastics with a significant proportion of branched polymers and enhanced aromatisation reactions may generate polyaromatic coke, which blocks the pores of HY.

Fig. 5a further shows the product distribution obtained during the hydrocracking of mixed plastic waste over the various zeolite samples. As expected, HY with the microporous structure showed the maximum selectivity of heavier oils and ≥ $C19^{+}$ (47.2 %), with low affinity

towards C_5-C_{18} (25.7 %). However, ST-HY with slightly better textural properties improved the selectivity of C_5-C_{18} (32.3 %), whereas CT-HY-1 showed a prominent amplification towards gasoline and diesel range hydrocarbons (50.1 %) at the expense of heavier oils (10.3 %). In contrast, CT-HY-2 with the maximum textural properties exhibited the highest selectivity of C_5-C_{18} (54 %), suggesting the dominant role of enhanced mesoporosity in providing the maximum accessibility to heavier oils towards the active sites in the zeolite framework. As a result, CT-HY-2 displayed the lowest selectivity towards heavier oils (9.5 %).

Moreover, in terms of product quality, all the zeolite samples showed high selectivity towards paraffins over cyclic hydrocarbons (Fig. 5c). Overall, HY presented high selectivity of iso-paraffins (50.3%), with an iso-/n-paraffin ratio of 3. Similarly, ST-HY achieved high iso-/n-paraffin ratios (3.3), with comparable selectivity of naphthenes to that of HY. This significant improvement in the iso-/n-paraffin ratios as compared to what has been observed before for the HDPE hydrocracking is due to the presence of branched-chain polymers (i.e., PP and LDPE) in the feedstock. This confirmed that branched-chain polymers were initially cracked over the external surface of zeolite, originating smaller fragments of iso-paraffins. However, their further cracking was restricted by the diffusional constraints caused by the HY and ST-HY. Contrary to this, top-down hierarchically modified zeolite samples showed iso-/n-paraffin ratios of 3.8–4.1, very much similar to those obtained with the virgin HDPE. This could be due to the better accessibility of CT-HY zeolites as compared to HY and ST-HY, thereby leading to the cracking of the isomerised species before these appeared in the final product. In addition, CT-HY-2, with the maximum porosity, showed the highest selectivity of naphthenes (12.5 %), owing to the fast reaction and diffusion rate as compared to other zeolite samples. However, the selectivity of aromatics virtually remained the same (20–25 %), which could be due to the presence of PS as its transformation renders almost exclusively aromatics [6], resulting in high selectivity of aromatics.

Furthermore, the sustainability analysis showed the environmental (-0.41 kg CO_2e kg_{feed}^{-1}) and economic benefits (0.48 \$ kg_{feed}^{-1}) of CT-HY-2 as compared to the other zeolite samples, confirming the importance of high textural properties of hierarchical zeolite towards achieving better results for the hydrocracking of mixed plastic waste (Fig. S7c–d). As a result, CT-HY-2 showed a 27 % improvement in the pareto front optimisation results as compared to HY (Fig. 5d).

To conclude, CT-HY-2 showed the highest conversion results and selectivity of lighter oils during the hydrocracking of mixed waste plastics, clarifying the role of improved and open mesoporosity in providing better diffusion and accessibility to the active sites of the zeolites when in presence of polymers containing branched structures. Similarly, the same catalyst showed the highest selectivity of middle distillate, iso−/n-paraffin ratio, and the maximum normalised score. This shows the potential of top-down hierarchically modified Y zeolite (CT-HY-2) for the impurity tolerated hydrocracking of mixed post-consumer plastic waste.

4.4. Sustainability analysis and comparison with previous literature

The principles of green chemistry emphasise sustainability by promoting energy-efficient processes with maximum efficiency, while keeping the environmental and operating expenses at a minimum value [62]. In the context of hydrocracking, a high catalytic conversion of plastic waste to economically viable products is needed, in order to follow the principle of green chemistry. However, the sustainability of the process is subject to the reaction conditions (i.e., reaction time, temperature, and hydrogen pressure), along with the environmental impact, and economic cost of the employed catalysts. For instance, prolonged reaction time and/or high reaction temperatures may improve the reaction rate at the expense of energy consumption. Similarly, the use of noble metals and expensive surfactants may compromise the sustainability of synthesized hierarchical zeolites. As a result, optimized reaction conditions and use of environmentally friendly and cost-effective catalysts are required to truly achieve a sustainable process.

Therefore, to assess the catalytic performance, the results of hierarchical zeolites obtained during the hydrocracking of mixed post-consumer plastic waste were compared with recent studies (Fig. 6a). A detailed discussion is part of SI (Table S9). However, it is worth noting that its quite challenging to directly compare the results from different studies discussing the hydrocracking of plastics under diverse reaction conditions (i.e., temperature, time, hydrogen pressure etc.). This complexity might make it difficult, or even inaccurate, to compare particular values among different studies. Therefore, rather than comparing specific values, a comparison is made based on the productivity of middle distillates ($g_{C5\text{-}C18}\ g_{cat}^{-1}\ h^{-1}$). This might be due to the fact that both gasoline and diesel range hydrocarbons showed better environmental and economic benefits as compared to gaseous products and heavier oils. Such comparative analyses have already been conducted by other researchers [6,55]. Overall, both top-down hierarchically modified zeolite samples showed high productivity of middle distillates, surpassing the previously reported values. However, most of these studies only performed the hydrocracking of low molecular weight virgin materials for a prolonged reaction time. For instance, Nakaji et al. [63] studied the hydrocracking of LPDE (Mw = 4000 g/mol) over Ru/CeO_2 (8 h) and Pt/HUSY (24 h) under 60 bar cold H_2 pressure at 240 °C and 260 °C respectively. Despite the intense reaction conditions (i.e., prolonged reaction time and hydrogen pressure), both catalysts showed low productivity of C_5-C_{18}. Similar results were reported by Qiu et al. [64], who performed the hydrocracking experiments of waste pipettes at 250 °C for 6 h under 25 bar cold hydrogen pressure. Also, both Liu et al. [32] and Zhang et al. [65] reported the low productivity of middle distillates while studying the hydrocracking of HDPE. Similarly, Zhang et al. [65] performed the hydrocracking of mixed post-consumer plastic waste over Ni-Hbeta at 250 °C for 20 h under 30 bar cold H_2 pressure. Interestingly, the catalyst showed higher conversion (>80 %) of mixed plastic waste into lighter oils, however the prolonged reaction time significantly reduced the productivity of middle distillates to 0.6 $g_{C5\text{-}C18}\ g_{cat}^{-1}\ h^{-1}$. Contrary to this, Munir et al. [66], achieved relatively higher productivity results (6–6.3 $g_{C5\text{-}C18}\ g_{cat}^{-1}\ h^{-1}$) at 360 °C, suggesting the dominant role of high reaction temperature over reaction time in achieving high productivity results. Therefore, by leveraging the reaction temperature rather than reaction time, we achieved high productivity of C_5-C_{18} products with the maximum value achieved over CT-HY-2 (8.35 $g_{C5\text{-}C18}\ g_{cat}^{-1}\ h^{-1}$).

Furthermore, Fig. 6b compares the environmental impact in terms of global warming potential (kg CO_2e g_{cat}^{-1}) for the synthesis of the various zeolite samples with the previous literature. The life cycle inventory and life cycle interpretation data are shown in Tables S1 and S3, whereas the quantification of previous literature is done by calculating the quantity of precursors and materials defined in the respective studies. Similarly, the impact assessment of commercial zeolites used for the post-synthesis modifications was assumed to be the same as that of HY in present study. Overall, both parent and hierarchically modified zeolite samples showed comparable results with the maximum impact over ST-HY (0.31 kg CO_2e g_{cat}^{-1}), owing to a prolonged crystallization time (72 h). However, the calculated impact is relatively lower as compared to other hierarchical techniques. For instance, Abdulridha et al. [41] synthesized an hierarchical Y zeolite (MY-CNT) using hard templating approach, exhibiting a high impact on global warming potential (0.67 kg CO_2e g_{cat}^{-1}). The high environmental impact was associated to the pre-treatment (i.e., oxidation) of the hard template material prior to the synthesis of the zeolite. Similarly, a two-step hierarchical modification (i.e., dealumination followed by desilication) of Y zeolite (MY-HT) showed a global warming potential of 0.35 kg CO_2e g_{cat}^{-1}. Similar results were observed for the top-down synthesis, where the dealumination of zeolite (DAHY-HCl) by acid leaching showed a slightly higher impact of 0.33 kg CO_2e g_{cat}^{-1} as compared to templating methods [5]. Fig. S8a further presents the sensitivity analysis based on sensitivity ratio of environmental impact for zeolite precursors across different zeolite types.

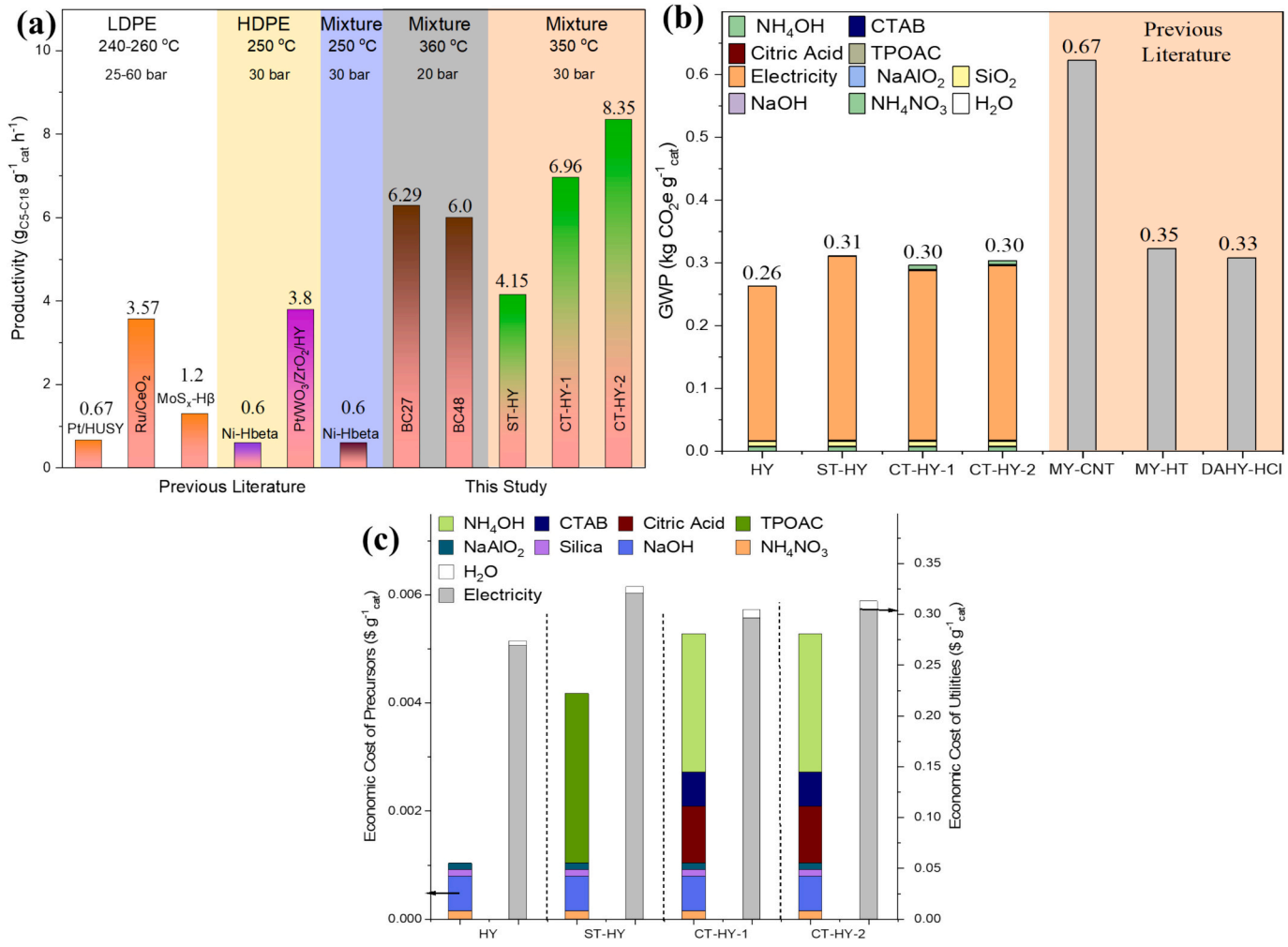

Fig. 6. (a) Productivity comparison of the present study for the hydrocracking of mixed post-consumer plastics waste with the previous literature. Both Pt/HUSY and Ru/CeO_2, MoS_x-HBeta, Ni-Hbeta, $Pt/WO_3/ZrO_2$/HY, Ni-Hbeta, and both BC27 and BC48 correspond to ref. [63], ref. [64], ref. [65], ref. [32], ref. [65] and ref. [66] respectively; (b) comparison of environmental impact associated with the synthesis of various zeolite samples in terms of their global warming potential (kg CO_2e g^{-1}_{cat}); and (c) comparison of economic cost ($ g^{-1}_{cat})associated for the synthesis of studied zeolite samples.

Moreover, Fig. 6c compares the economic cost ($ g^{-1}_{cat}) for the synthesis of various zeolite samples in laboratory settings. The cost of individual precursors and materials is listed in Tables S2 and S3. Overall, parent HY zeolite showed the least cost of 0.28 $ g^{-1}_{cat}. However, the use of an expensive template (TPOAC) and prolonged crystallization time increased the cost of ST-HY (0.33 $ g^{-1}_{cat}), whereas both CT-HY samples showed similar costs associated with synthesizing surfactant templating zeolites. The calculated values are significantly lower than the economic cost of hierarchical zeolites prepared by acid leaching and hard templating as discussed in SI (Fig. S8b). Moreover, keeping in mind the variation of the precursor costs among different studies and vendors, we performed the sensitivity analysis (± 20 %) based on the change of each single precursor (Fig. S8c).

Briefly, for the synthesis of HY, a variation of 20 % of NaOH cost significantly change the overall cost of catalyst, whereas ST-HY exhibited the maximum sensitivity towards the cost of TPOAC (SR = 0.75 %). In contrast, both top-down hierarchical zeolite samples showed the maximum sensitivity towards the variation in the cost of ammonium hydroxide solution (SR = 0.49 %).

To conclude, the current study highlighted an alternative framework to compare the sustainability of the developed catalysts by comparing their environmental and economic impacts associated to their synthesis and modification routes. Similarly, the results of the studied zeolite samples were compared with the previous literature based on the productivity of middle distillate. Overall, the top-down hierarchical modification of Y zeolite via surfactant-templating showed high productivity of gasoline and diesel range hydrocarbons. Also, both CT-HY samples exhibited lower environmental impact (kg CO_2e g^{-1}_{cat}) and showed economic benefits during synthesis, confirming their great potential for the hydrocracking of plastics.

5. Conclusion

This study compares the pore-structure accessibility of various hierarchical HY zeolites towards the hydrocracking of linear and branched plastics. Compared to HY, all the hierarchical zeolites exhibited an increase in the conversion of HDPE, a linear plastic, in line with their conversion factor, confirming the collective contribution of the textural and acidic properties for better catalytic performance. Top-down hierarchically modified HY zeolites (CT-HY) showed the best HDPE conversions and selectivity of lighter oils owing to their significantly higher mesoporosity and acidity strength. However, it was verified that while gasoline product quality progressively enhances with mesoporosity development, HDPE conversion stabilises after a certain threshold in the generation of mesopores. In terms of environmental and economic benefits, both CT-HY zeolite samples significantly surpassed the benefits achieved over HY and ST-HY due to their high activity results. Conversely, a different conversion trend was observed during the

hydrocracking of mixed post-consumer plastic waste, containing linear and branched polymers, with conversion increasing with the increase in mesoporous volume. This clearly shows the impact of improved structure accessibility to the conversion of more voluminous, branched, plastic wastes, as compared to linear plastic wastes. As a result, CT-HY-2 displayed the maximum selectivity (73.8 %) and productivity (8.4 $g_{C5\text{-}C12}\ g_{cat}^{-1}\ h^{-1}$) of middle distillates. Similarly, it showed the highest environmental (−0.41 kg CO_2e kg_{feed}^{-1}) and economic benefits (0.48 \$ kg_{feed}^{-1}), with a 27 % higher Pareto front optimisation score as compared to HY. Finally, the sustainability analysis of hierarchically modified zeolite samples showed that the synthesis of both top-down templated zeolites resulted in relatively lower environmental and economic impact as compared to bottom-up templated zeolite (ST-HY), suggesting the more sustainable nature of the former. Overall, this work sheds light into the impact of mesoporosity on the conversion of linear and branched plastics and on product quality. Unlike the conventional comparison purely based on activity and selectivity values, the Pareto front optimisation, by considering the normalised score of conversion and environmental and economic benefits, additionally provided an insight to the sustainable design and comparison of different catalysts.

CRediT authorship contribution statement

Muhammad Usman Azam: Writing – original draft, Investigation, Conceptualization. **Nanbyen George Kim:** Investigation. **Auguste Fernandes:** Writing – review & editing, Investigation. **M. Filipa Ribeiro:** Writing – review & editing. **Waheed Afzal:** Writing – review & editing, Supervision, Conceptualization. **Inês Graça:** Writing – review & editing, Supervision, Conceptualization.

Declaration of competing interest

The authors declare that they have no known competing financial interests or personal relationships that could have appeared to influence the work reported in this paper.

Acknowledgements

This study was funded by The LEVERHULME TRUST (Grant DS-2017-073). Muhammad Usman Azam, a Leverhulme Trust Doctoral Scholar, was part of the 15 PhD scholarships of the “Leverhulme Centre for Doctoral Training in Sustainable Production of Chemicals and Materials” at the University of Aberdeen (Scotland, United Kingdom). Nanbyen George Kim thanks the Petroleum Technology Development Fund (PTDF) for sponsoring her PhD scholarship (PTDF/ED/OSS/PHD/NS/2045/22 - 22PHD097). Auguste Fernandes thanks Portuguese FCT for funding (CQE - UIDB/00100/2020 and UIDP/00100/2020; IMS - LA/P/0056/2020; contract hiring under DL57/2016 law). The authors also acknowledge Dr Alan McCue (University of Aberdeen, UK) and Gillian Milne (Senior Histology Technician, UoA) for providing technical support during catalyst characterizations.

Appendix A. Supplementary data

Supplementary data to this article can be found online at https://doi.org/10.1016/j.cej.2025.172045.

Data availability

The data supporting this article have been included as part of the Supplementary information.

References

[1] A.S. Pottinger, R. Geyer, N. Biyani, C.C. Martinez, N. Nathan, M.R. Morse, C. Liu, S. Hu, M. de Bruyn, C. Boettiger, Pathways to reduce global plastic waste mismanagement and greenhouse gas emissions by 2050, Science 386 (6726) (2024) 1168–1173.
[2] K.D. Nixon, Z.O. Schyns, Y. Luo, M.G. Ierapetritou, D.G. Vlachos, L.T. Korley, I. Epps, H. Thomas, Analyses of circular solutions for advanced plastics waste recycling, Nat. Chem. Eng. 1 (10) (2024) 615–626.
[3] H. Li, H.A. Aguirre-Villegas, R.D. Allen, X. Bai, C.H. Benson, G.T. Beckham, S. L. Bradshaw, J.L. Brown, R.C. Brown, V.S. Cecon, Expanding plastics recycling technologies: chemical aspects, technology status and challenges, Green Chem. 24 (23) (2022) 8899–9002.
[4] B. Hernández, D.G. Vlachos, M.G. Ierapetritou, Superstructure optimization for management of low-density polyethylene plastic waste, Green Chem. 26 (17) (2024) 9476–9487.
[5] M.U. Azam, W. Afzal, A. Fernandes, I. Graça, Insights into the development of greener mild zeolite dealumination routes applied to the hydrocracking of waste plastics, Appl. Catal. A Gen. 685 (2024) 119873.
[6] M.U. Azam, A. Fernandes, M.J. Ferreira, W. Afzal, I. Graça, Pore-structure engineering of hierarchical β zeolites for the enhanced hydrocracking of waste plastics to liquid fuels, ACS Catal. 14 (2024) 16148–16165.
[7] M.U. Azam, A. Fernandes, M.J. Ferreira, A.J. McCue, I. Graça, W. Afzal, Unlocking the structure-activity relationship of hierarchical MFI zeolites towards the hydrocracking of HDPE, Fuel 379 (2025) 132990.
[8] M.U. Azam, W. Afzal, I. Graça, Advancing plastic recycling: a review on the synthesis and applications of hierarchical zeolites in waste plastic hydrocracking, Catalysts 14 (7) (2024) 450.
[9] W. Han, L. Lin, Z. Cen, Y. Ke, Q. Xu, J. Zhu, X. Mei, Z. Xia, X. Zheng, Y. Wang, Production of branched alkanes by upcycling of waste polyethylene over controlled acid sites of SO4/ZrO2-Al2O3 catalyst, Angew. Chem. 137 (6) (2025) e202417923.
[10] Z. Cen, X. Han, L. Lin, S. Yang, W. Han, W. Wen, W. Yuan, M. Dong, Z. Ma, F. Li, Upcycling of polyethylene to gasoline through a self-supplied hydrogen strategy in a layered self-pillared zeolite, Nat. Chem. 16 (6) (2024) 871–880.
[11] X. Zhou, X. Han, Z. Qu, J. Zhang, F. Zeng, Z. Tang, R. Chen, Hierarchical FAU zeolites boosting the hydrocracking of polyolefin waste into liquid fuels, ACS Sustain. Chem. Eng. 12 (15) (2024) 6013–6022.
[12] A. Gacem, K.K. Yadav, M. Khalid, H.A. Alqhtani, M. Bin-Jumah, C. Kavitha, P. Tamizhdurai, Green energy production: hydroprocessing of waste plastic to diesel fuel using bimetal of Mn/Zn supported on activated carbon, RSC Adv. 15 (10) (2025) 7769–7785.
[13] Y.-Y. Wang, A. Tennakoon, X. Wu, C. Sahasrabudhe, L. Qi, B.G. Peters, A.D. Sadow, W. Huang, Catalytic hydrogenolysis of polyethylene under reactive separation, ACS Catal. 14 (3) (2024) 2084–2094.
[14] J.A. Sun, P.A. Kots, Z.R. Hinton, N.S. Marinkovic, L. Ma, S.N. Ehrlich, W. Zheng, T. H. Epps III, L.T. Korley, D.G. Vlachos, Size and structure effects of carbon-supported ruthenium nanoparticles on waste polypropylene hydrogenolysis activity, selectivity, and product microstructure, ACS Catal. 14 (5) (2024) 3228–3240.
[15] H. Raghav, B. Joshi, K.L. Kumar, S. Kumar, B. Sarkar, Catalytic pyrolysis of low-density waste polyethylene into light olefins and hydrogen over manganese-supported alumina, J. Environ. Chem. Eng. 13 (1) (2025) 115254.
[16] P. Zhao, W. Guo, Z. Gui, J. Jiang, Z. Zhu, J.-J. Li, L. Zhao, J. Zhou, Z. Xi, Selective hydrocracking of waste polyolefins toward gasoline-range liquid fuels via tandem catalysis over a cerium-promoted Pt/HY catalyst, ACS Sustain. Chem. Eng. 12 (15) (2024) 5738–5752.
[17] J.Z. Tan, M. Ortega, S.A. Miller, C.W. Hullfish, H. Kim, S. Kim, W. Hu, J.Z. Hu, J. A. Lercher, B.E. Koel, Catalytic consequences of hierarchical pore architectures within MFI and FAU zeolites for polyethylene conversion, ACS Catal. 14 (10) (2024) 7536–7552.
[18] Z. Dong, W. Chen, K. Xu, Y. Liu, J. Wu, F. Zhang, Understanding the structure–activity relationships in catalytic conversion of polyolefin plastics by zeolite-based catalysts: a critical review, ACS Catal. 12 (24) (2022) 14882–14901.
[19] V. Valtchev, G. Majano, S. Mintova, J. Pérez-Ramírez, Tailored crystalline microporous materials by post-synthesis modification, Chem. Soc. Rev. 42 (1) (2013) 263–290.
[20] L.-H. Chen, M.-H. Sun, Z. Wang, W. Yang, Z. Xie, B.-L. Su, Hierarchically structured zeolites: from design to application, Chem. Rev. 120 (20) (2020) 11194–11294.
[21] M.P. González-Marcos, E.G. Fuentes-Ordóñez, J.A. Salbidegoitia, J.R. González-Velasco, Optimization of supports in bifunctional supported Pt catalysts for polystyrene hydrocracking to liquid fuels, Top. Catal. 64 (2021) 224–242.
[22] S. Tsubota, S. Kokuryo, K. Miyake, Y. Uchida, A. Mizusawa, T. Kubo, N. Nishiyama, Understanding the role of the surface acidity of MFI zeolites during LDPE cracking: decomposition temperature and product distribution, ACS Catal. 14 (23) (2024) 18145–18155.
[23] K. Pyra, K.A. Tarach, D. Majda, K. Góra-Marek, Desilicated zeolite BEA for the catalytic cracking of LDPE: the interplay between acidic sites' strength and accessibility, Cat. Sci. Technol. 9 (8) (2019) 1794–1801.
[24] S. Armenise, C.S. Costa, W.S. Luing, M.R. Ribeiro, J.M. Silva, T. Onfroy, L. Valentin, S. Casale, M. Muñoz, F. Launay, Evaluation of two approaches for the synthesis of hierarchical micro-/mesoporous catalysts for HDPE hydrocracking, Microporous Mesoporous Mater. 356 (2023) 112605.
[25] P.A. Kots, P.A. Doika, B.C. Vance, S. Najmi, D.G. Vlachos, Tuning high-density polyethylene hydrocracking through mordenite zeolite crystal engineering, ACS Sustain. Chem. Eng. 11 (24) (2023) 9000–9009.
[26] C.H. Tempelman, X. Zhu, K. Gudun, B. Mezari, B. Shen, E.J. Hensen, Texture, acidity and fluid catalytic cracking performance of hierarchical faujasite zeolite prepared by an amphiphilic organosilane, Fuel Process. Technol. 139 (2015) 248–258.

[27] A. Sachse, A. Grau-Atienza, E.O. Jardim, N. Linares, M. Thommes, J. Garcia-Martinez, Development of intracrystalline mesoporosity in zeolites through surfactant-templating, Cryst. Growth Des. 17 (8) (2017) 4289–4305.
[28] M. Choi, K. Na, J. Kim, Y. Sakamoto, O. Terasaki, R. Ryoo, Stable single-unit-cell nanosheets of zeolite MFI as active and long-lived catalysts, Nature 461 (7261) (2009) 246–249.
[29] G. Song, W. Chen, P. Dang, S. Yang, Y. Zhang, Y. Wang, R. Xiao, R. Ma, F. Li, Synthesis and characterization of hierarchical ZSM-5 zeolites with outstanding mesoporosity and excellent catalytic properties, Nanoscale Res. Lett. 13 (1) (2018) 364.
[30] R. García, D. Serrano, D. Otero, Catalytic cracking of HDPE over hybrid zeolitic–mesoporous materials, J. Anal. Appl. Pyrolysis 74 (1–2) (2005) 379–386.
[31] C.S. Costa, M. Muñoz, M.R. Ribeiro, J.M. Silva, H-USY and H-ZSM-5 zeolites as catalysts for HDPE conversion under a hydrogen reductive atmosphere, Sustain. Energy Fuels 5 (4) (2021) 1134–1147.
[32] S. Liu, P.A. Kots, B.C. Vance, A. Danielson, D.G. Vlachos, Plastic waste to fuels by hydrocracking at mild conditions, Sci. Adv. 7 (17) (2021) eabf8283.
[33] M. Muñoz, I. Morales, C.S. Costa, M. Multigner, P. De La Presa, J.M. Alonso, J. M. Silva, M.d.R. Ribeiro, B. Torres, J. Rams, Local induction heating capabilities of zeolites charged with metal and oxide MNPs for application in HDPE hydrocracking: a proof of concept, Materials 14 (4) (2021) 1029.
[34] D. Perera, L. Amarasena, V. Madhusanka, X. Chen, R. Weerasooriya, A. Bandara, L. Jayarathna, Enhancing the understanding of surfactant influence in LTA crystallization through microwave-assisted methods at different temperatures, J. Porous. Mater. 32 (3) (2025) 1003–1026.
[35] A. Al-Ani, J.J. Haslam, N.E. Mordvinova, O.I. Lebedev, A. Vicente, C. Fernandez, V. Zholobenko, Synthesis of nanostructured catalysts by surfactant-templating of large-pore zeolites, Nanoscale Adv. 1 (5) (2019) 2029–2039.
[36] N. Linares, A. Sachse, E. Serrano, A. Grau-Atienza, E. De Oliveira Jardim, J. Silvestre-Albero, M.A.L. Cordeiro, F. Fauth, G. Beobide, O. Castillo, In situ time-resolved observation of the development of intracrystalline mesoporosity in USY zeolite, Chem. Mater. 28 (24) (2016) 8971–8979.
[37] W. Lutz, Zeolite Y: synthesis, modification, and properties—a case revisited, Adv. Mater. Sci. Eng. 2014 (1) (2014) 724248.
[38] T.H. Vuong, N. Rockstroh, U. Bentrup, J. Rabeah, J. Knossalla, S. Peitz, R. Franke, A. Brückner, Role of surface acidity in formation and performance of active Ni single sites in supported catalysts for butene dimerization: a view inside by operando EPR and in situ FTIR spectroscopy, ACS Catal. 11 (6) (2021) 3541–3552.
[39] Y. Zhou, A. Galarneau, J. Rodriguez, M. Opanasenko, M. Shamzhy, Correlating mesoporosity/acidity with catalytic performances for surfactant-templated mesoporous FAU zeolites, Mater. Adv. 5 (8) (2024) 3207–3219.
[40] W. Fu, L. Zhang, T. Tang, Q. Ke, S. Wang, J. Hu, G. Fang, J. Li, F.-S. Xiao, Extraordinarily high activity in the hydrodesulfurization of 4, 6-dimethyldibenzothiophene over Pd supported on mesoporous zeolite Y, J. Am. Chem. Soc. 133 (39) (2011) 15346–15349.
[41] S. Abdulridha, Y. Jiao, S. Xu, R. Zhang, Z. Ren, A.A. Garforth, X. Fan, A comparative study on mesoporous Y zeolites prepared by hard-templating and post-synthetic treatment methods, Appl. Catal. A Gen. 612 (2021) 117986.
[42] M.H. Sun, L.H. Chen, S. Yu, Y. Li, X.G. Zhou, Z.Y. Hu, Y.H. Sun, Y. Xu, B.L. Su, Micron-sized zeolite beta single crystals featuring intracrystal interconnected ordered macro-meso-microporosity displaying superior catalytic performance, Angew. Chem. 132 (44) (2020) 19750–19759.
[43] A. Ruggiu, A.P. Carvalho, E. Rombi, A. Martins, J. Rocha, P. Parpot, I.C. Neves, M. G. Cutrufello, Y and ZSM-5 hierarchical zeolites prepared using a surfactant-mediated strategy: effect of the treatment conditions, Materials 17 (17) (2024) 4401.
[44] J. Zhao, Y. Yin, Y. Li, W. Chen, B. Liu, Synthesis and characterization of mesoporous zeolite Y by using block copolymers as templates, Chem. Eng. J. 284 (2016) 405–411.
[45] K. Li, J. Valla, J. Garcia-Martinez, Realizing the commercial potential of hierarchical zeolites: new opportunities in catalytic cracking, ChemCatChem 6 (1) (2014) 46–66.
[46] K. Pyra, K.A. Tarach, A. Śrębowata, I. Melián-Cabrera, K. Góra-Marek, Pd-modified beta zeolite for modulated hydro-cracking of low-density polyethylene into a paraffinic-rich hydrocarbon fuel, Appl. Catal. B Environ. 277 (2020) 119070.
[47] M. Milina, S. Mitchell, N.-L. Michels, J. Kenvin, J. Pérez-Ramírez, Interdependence between porosity, acidity, and catalytic performance in hierarchical ZSM-5 zeolites prepared by post-synthetic modification, J. Catal. 308 (2013) 398–407.
[48] B. Puértolas, A. Veses, M.S. Callén, S. Mitchell, T. García, J. Pérez-Ramírez, Porosity–acidity interplay in hierarchical ZSM-5 zeolites for pyrolysis oil valorization to aromatics, ChemSusChem 8 (19) (2015) 3283–3293.
[49] S. Müller, Y. Liu, F.M. Kirchberger, M. Tonigold, M. Sanchez-Sanchez, J.A. Lercher, Hydrogen transfer pathways during zeolite catalyzed methanol conversion to hydrocarbons, J. Am. Chem. Soc. 138 (49) (2016) 15994–16003.
[50] L. Li, H. Luo, Z. Shao, H. Zhou, J. Lu, J. Chen, C. Huang, S. Zhang, X. Liu, L. Xia, Converting plastic wastes to naphtha for closing the plastic loop, J. Am. Chem. Soc. 145 (3) (2023) 1847–1854.
[51] F.J. Vela, R. Palos, J.R. García, U. Sedran, J. Bilbao, J.M. Arandes, A. Gutiérrez, Enhancing the performance of a PtPd/HY catalyst for HDPE/VGO hydrocracking through zeolite desilication, Fuel 329 (2022) 125392.
[52] M.U. Azam, A. Vete, W. Afzal, Process simulation and life cycle assessment of waste plastics: a comparison of pyrolysis and hydrocracking, Molecules 27 (22) (2022) 8084.
[53] B. Hernández, P. Kots, E. Selvam, D.G. Vlachos, M.G. Ierapetritou, Techno-economic and life cycle analyses of thermochemical upcycling technologies of low-density polyethylene waste, ACS Sustain. Chem. Eng. 11 (18) (2023) 7170–7181.
[54] V. Cappello, P. Sun, G. Zang, S. Kumar, R. Hackler, H.E. Delgado, A. Elgowainy, M. Delferro, T. Krause, Conversion of plastic waste into high-value lubricants: techno-economic analysis and life cycle assessment, Green Chem. 24 (16) (2022) 6306–6318.
[55] B.C. Vance, Z. Yuliu, S. Najmi, E. Selvam, J.E. Granite, K. Yu, M.G. Ierapetritou, D. G. Vlachos, Unlocking naphtha from polyolefins using Ni-based hydrocracking catalysts, Chem. Eng. J. 487 (2024) 150468.
[56] Y. Miao, Y. Zhao, G.I. Waterhouse, R. Shi, L.-Z. Wu, T. Zhang, Photothermal recycling of waste polyolefin plastics into liquid fuels with high selectivity under solvent-free conditions, Nat. Commun. 14 (1) (2023) 4242.
[57] A. Marcilla, A. Gómez-Siurana, F. Valdés, Influence of the temperature on the composition of the coke obtained in the catalytic cracking of low density polyethylene in the presence of USY and HZSM-5 zeolites, Microporous Mesoporous Mater. 109 (1–3) (2008) 420–428.
[58] M. Díaz, E. Epelde, J. Valecillos, S. Izaddoust, A.T. Aguayo, J. Bilbao, Coke deactivation and regeneration of HZSM-5 zeolite catalysts in the oligomerization of 1-butene, Appl. Catal. B Environ. 291 (2021) 120076.
[59] Y. Wang, N. Yan, Z. Chen, Identification of coke species on Fe/USY catalysts used for recycling polyethylene into fuels, RSC Adv. 14 (31) (2024) 22056–22062.
[60] A. bin Jumah, A.A. Tedstone, A.A. Garforth, Hydrocracking of virgin and post-consumer polymers, Microporous Mesoporous Mater. 315 (2021) 110912.
[61] M. Ibáñez, M. Artetxe, G. Lopez, G. Elordi, J. Bilbao, M. Olazar, P. Castaño, Identification of the coke deposited on an HZSM-5 zeolite catalyst during the sequenced pyrolysis–cracking of HDPE, Appl. Catal. B Environ. 148 (2014) 436–445.
[62] S.L. Tang, R.L. Smith, M. Poliakoff, Principles of green chemistry: productively, Green Chem. 7 (11) (2005) 761–762.
[63] Y. Nakaji, M. Tamura, S. Miyaoka, S. Kumagai, M. Tanji, Y. Nakagawa, T. Yoshioka, K. Tomishige, Low-temperature catalytic upgrading of waste polyolefinic plastics into liquid fuels and waxes, Appl. Catal. B Environ. 285 (2021) 119805.
[64] Z. Qiu, S. Lin, Z. Chen, A. Chen, Y. Zhou, X. Cao, Y. Wang, B.-L. Lin, A reusable, impurity-tolerant and noble metal–free catalyst for hydrocracking of waste polyolefins, Sci. Adv. 9 (25) (2023) eadg5332.
[65] G. Zhang, Q. Mao, Y. Yue, R. Gao, Y. Duan, H. Du, Ni-based catalysts supported on Hbeta zeolite for the hydrocracking of waste polyolefins, RSC Adv. 14 (23) (2024) 15856–15861.
[66] D. Munir, H. Amer, R. Aslam, M. Bououdina, M.R. Usman, Composite zeolite beta catalysts for catalytic hydrocracking of plastic waste to liquid fuels, Mater. Renew. Sustain. Energy 9 (2020) 1–13.